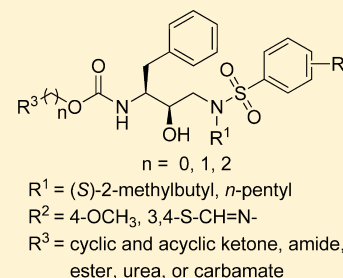


Design, Synthesis, and Biological and Structural Evaluations of Novel HIV-1 Protease Inhibitors To Combat Drug Resistance

Maloy Kumar Parai,[†] David J. Huggins,[‡] Hong Cao,[§] Madhavi N. L. Nalam,^{||} Akbar Ali,[§] Celia A. Schiffer,^{||} Bruce Tidor,[‡] and Tariq M. Rana^{*,†,§}[†]Program for RNA Biology, Sanford-Burnham Medical Research Institute, La Jolla, California 92037, United States[‡]Department of Biological Engineering and Computer Science and Artificial Intelligence Laboratory, Massachusetts Institute of Technology, Cambridge, Massachusetts 02139, United States[§]Chemical Biology Program, Department of Biochemistry and Molecular Pharmacology, University of Massachusetts Medical School, Worcester, Massachusetts 01605, United States^{||}Department of Biochemistry and Molecular Pharmacology, University of Massachusetts Medical School, Worcester, Massachusetts 01605, United States

Supporting Information

ABSTRACT: A series of new HIV-1 protease inhibitors (PIs) were designed using a general strategy that combines computational structure-based design with substrate-envelope constraints. The PIs incorporate various alcohol-derived P2 carbamates with acyclic and cyclic heteroatomic functionalities into the (*R*)-hydroxyethylamine isostere. Most of the new PIs show potent binding affinities against wild-type HIV-1 protease and three multidrug resistant (MDR) variants. In particular, inhibitors containing the 2,2-dichloroacetamide, pyrrolidinone, imidazolidinone, and oxazolidinone moieties at P2 are the most potent with K_i values in the picomolar range. Several new PIs exhibit nanomolar antiviral potencies against patient-derived wild-type viruses from HIV-1 clades A, B, and C and two MDR variants. Crystal structure analyses of four potent inhibitors revealed that carbonyl groups of the new P2 moieties promote extensive hydrogen bond interactions with the invariant Asp29 residue of the protease. These structure–activity relationship findings can be utilized to design new PIs with enhanced enzyme inhibitory and antiviral potencies.



INTRODUCTION

The human immunodeficiency virus type 1 (HIV-1) protease plays an important role in the viral replication by processing the viral Gag and Gag-Pol polyproteins into functional and structural proteins essential for viral assembly and maturation. Inhibition of HIV-1 protease leads to the generation of immature virus particles. Hence, HIV-1 protease has emerged as a promising target for therapeutic intervention in HIV/AIDS patients. The addition of protease inhibitors (PIs) to the highly active antiretroviral therapy (HAART) with reverse-transcriptase inhibitors resulted in an unprecedented success of HIV/AIDS chemotherapy.^{1–4} However, rapid emergence of drug-resistant HIV-1 variants, transmission of these resistant viral strains, and the adverse effects of currently used HIV-1 PIs remain critical factors limiting the clinical effectiveness of antiretroviral therapies.^{5–7} Therefore, to alleviate these problems, there is a need for the development of new PIs with improved activity against drug resistant variants and excellent pharmacokinetic and safety profiles.

Crystal structure analyses of HIV-1 protease in complex with its peptide substrates suggest that substrate specificity depends on matching a defined shape within the binding site. This shape has been termed as the substrate envelope.⁸ Among the FDA approved PIs, amprenavir⁹ (**1**, APV, Figure 1) containing tetrahydrofuran (THF) as the P2 ligand fits reasonably well

within the substrate envelope. The structurally similar non-peptidic PI darunavir^{10–13} (**2**, DRV, Figure 1) with bis-tetrahydrofuran (bis-THF) as the P2 ligand exerts high in vitro and in vivo antiviral potency against wild-type HIV-1 as well as multidrug resistant (MDR) strains. It is reasoned that the additional interactions of bis-THF moiety in inhibitor **2** with the backbone atoms of Asp29 and Asp30 residues in protease result in its potent activity against MDR HIV-1 variants.^{13,14} However, inhibitor **2**, though significantly more potent than **1**, contains a structurally complex and stereochemically defined P2 ligand, requiring multiple steps for synthesis. In addition to inhibitor **2**, a number of highly potent PIs incorporate the bis-THF moiety or similar bicyclic ether and flexible polyether based P2 ligands that mimic bis-THF.^{15–20}

We have been pursuing a general strategy combining structure-based design with substrate-envelope constraints to develop novel HIV-1 PIs against clinically relevant MDR protease variants with reduced structural complexity and hence cost effectiveness. We have recently reported a series of novel PIs that incorporate stereochemically defined *N*-phenyl-oxazolidinone-5-carboxamides as P2 ligands into the (*R*)-(hydroxyethylamino)sulfonamide isostere, the core scaffold of

Received: February 23, 2012

Published: June 18, 2012

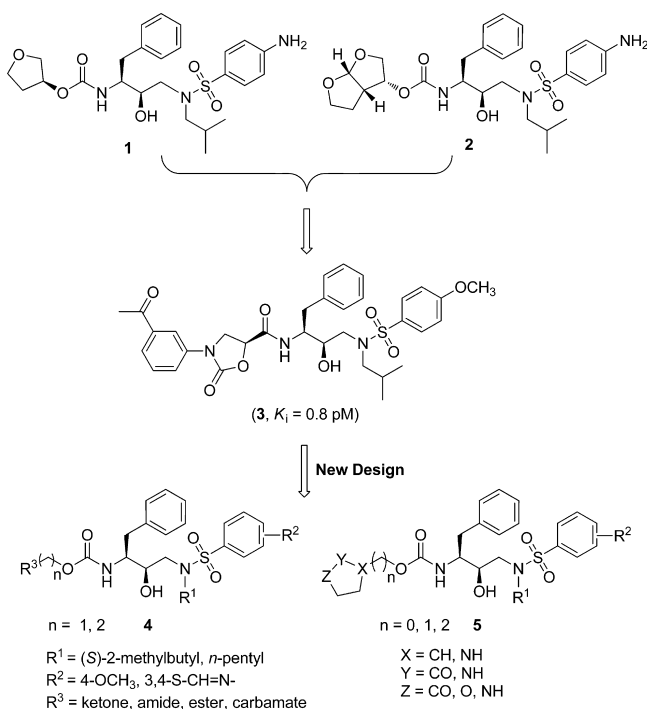


Figure 1. Chemical structures of amprevnavir **1**, darunavir **2**, lead compound **3**, and designed inhibitors **4** and **5**.

inhibitors **1** and **2**, and possess impressive enzyme affinities and antiviral activity against both wild-type and a panel of MDR HIV-1 variants.^{21,22} Moreover, crystal structure analysis of inhibitor **3** in complex with wild-type HIV-1 protease confirmed that the carbonyl group of the oxazolindione ring mimics the hydrogen-bond interactions of THF/bis-THF moieties of inhibitors **1** and **2**, respectively.

Since the carbonyl oxygen of ester, amide, and lactone functionalities can also act as hydrogen bond acceptors, it is expected that the above functionalities could mimic the critical hydrogen bonding interactions of bis-THF with the protease enzyme, and the presence of other heteroatoms in the ligand would make additional interactions with the side chain residues of the protease in the S2 binding pocket. Thus, we envisioned that P2 ligands containing ester, amide, urea, and lactone with flexible carbon chain may accommodate amino acid side chain variations and interact strongly with enzyme backbone. On the basis of this precept, we selected as P2 ligands alcohols **6a–j** containing structurally related five-membered heterocyclic structures pyrrolidone, dihydrofuranone, imidazolidone, and oxazolindione and some acyclic ketone, ester, amide subunits for the design of new PIs. To investigate the potential of these functionalized P2 ligands in combination with (*R*)-(hydroxyethylamino)sulfonamide isostere, we have designed and synthesized a series of new PIs (Figure 1).

In the present study, we report the structure-based computational design, synthesis, and biological evaluation of a series of HIV-1 PIs incorporating a variety of P2 carbamates derived from acyclic and cyclic alcohols. Structure–activity relationship (SAR) studies with variations at P2, P2', and P1' positions resulted in the generation of several highly potent HIV-1 PIs. Compounds with potent enzymatic activity have been further evaluated against a panel of MDR HIV-1 protease variants and for antiviral activity in cellular assays against patient derived wild-type HIV-1 viruses from clades A, B, and C

and two MDR HIV-1 variants. Crystal structures of the four most potent new inhibitors **13c**, **13g**, **13f**, and **14j** in complex with wild-type HIV-1 protease are also discussed.

COMPUTATIONAL DESIGN

The aim of inverse design is to consider a large combinatorial library of potential inhibitors and identify a set of molecules with high affinity against a protein target. The first step in the inverse design procedure is to select and prepare the protein target structure. Previous work on HIV-1 protease has shown that improved results can be achieved by using a crystal structure containing a ligand that is similar to the molecules in the combinatorial library.²³ The ligand is removed from the complex to yield a structure that is amenable for inverse design. In this work, based on the (*R*)-hydroxyethylamine isostere of inhibitors **1** and **2**, the 2-bound HIV-1 protease structure (PDB accession code 1T3R) was used.

Once selected, the protein structure was subjected to a standard preparation protocol. Coordinates were taken from the PDB, and the ligand was removed from the bound state. Three tightly bound water molecules (HOH1201, HOH1202, and HOH1203) were retained, with all other water molecules removed. The protein and water hydrogen-atom positions were then built using the HBUILD facility of the CHARMM27 program package²⁴ with the CHARMM22 energy function.²⁵ Histidine residues were checked for orientations and protonation state, which resulted in the two His69 residues being flipped and assigned as ϵ protonated. The residues lysine, arginine, aspartate, glutamate, cysteine, and tyrosine were also analyzed to check their protonation state. There was no evidence of any unusual protonation states, and thus, all lysine and arginine residues were assigned as positively charged, all aspartate and glutamate residues were assigned as negatively charged, and all cysteine and tyrosine residues were assigned as neutral. After minimization of the hydrogen-atom positions, the resultant structures were then rotated into a new coordinate frame and the protein atoms were assigned PARSE charges²⁶ for use with Delphi.^{27,28} The next stage involved creating van der Waals and electrostatic grids for grid-based energy calculations. The primary scoring function contains three components: a van der Waals term, a screened electrostatic interaction term, and desolvation penalties for the ligand and the protein. Grids for van der Waals energies are computed by placing every type of parametrized CHARMM atom type at each grid point and computing its van der Waals interaction energy with the protein. For any charged atoms at the grid points, the electrostatic binding free energy was calculated using the linearized Poisson–Boltzmann equation²⁹ using a locally modified version of the DelPhi computer program.³⁰

The next step in the inverse design procedure is to generate the volume in which the designed inhibitors must lie. During the attempt to design molecules that are not susceptible to resistance mutations, this volume is the substrate envelope. The substrate envelope is generated from the consensus volume of a set of naturally occurring substrates. In this case, the substrate envelope was created from five aligned HIV-1 protease–substrate peptide complexes and then transferred to a 2-bound HIV-1 protease structure.²³ After selection and preparation of the protein structure and the design shape, the next stage is to place the core scaffold in an ensemble of low-energy conformations within the site. The core scaffold in this case is the (*R*)-hydroxyethylamine isostere shown in Figure 1. A systematic set of conformations was created by rotating each

rotatable torsion angle in increments of 30°. Each conformation was then subjected to systematic placement in the active site with a translational enumeration of 0.25 Å and a rotational enumeration such that the maximum arc length of atoms from the centroid swept out a distance of 1.0 Å between orientations. Scaffold placements were accepted if all atom centers were contained within the substrate envelope but discarded if their calculated van der Waals binding energy was greater than zero or any two nonbonded atoms' 0.75-scaled radii overlapped.

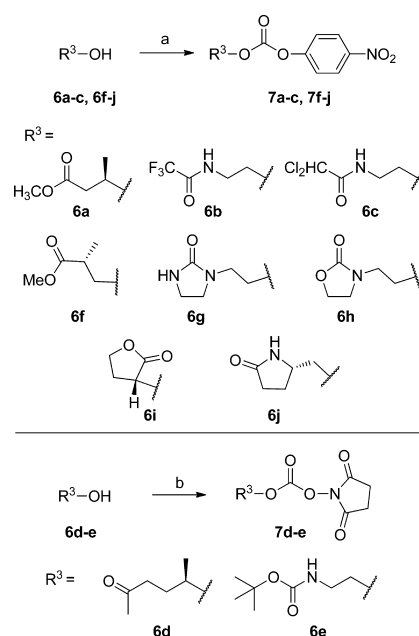
Each designed inhibitor comprises the (*R*)-hydroxyethylamine isostere with three side group substituents, termed R¹, R², and R³. These substituents are derived from primary amines, sulfonyl chlorides, and alcohols, respectively (Scheme 2). The substituents used in the inverse design procedure were taken from the ZINC database of commercially available compounds.³¹ Every acceptable scaffold pose was used for a separate design with the set of side group substituents at R¹, R², and R³ using the guaranteed combinatorial search algorithms dead-end elimination (DEE)³² and A*.³³ The DEE/A* algorithm places all side group substituents in all conformations and combinations on each scaffold pose to yield an energy-ranked list of 1000 unique molecules. The ranked list was then reduced to a computationally feasible size by removing compounds with an energy of 25.0 kcal/mol or higher than the lowest energy result. The resulting top-ranked compounds from the combinatorial search were re-evaluated using more accurate physics-based energy functions to identify candidate molecules for synthesis and testing. The most sophisticated energy function included a geometry optimization using CHARMM, performed on the ligand in a rigid protein structure for 1 000 000 steps using the adopted basis Newton–Raphson method. The binding free energies were then estimated using a molecular mechanics and Poisson–Boltzmann/surface area (MM-PB/SA) method.³⁰ This includes the sum of van der Waals interactions with the protein, an electrostatic binding free energy calculated by solving the linearized Poisson–Boltzmann equation in both the bound and unbound states, and the surface area burial term was multiplied by the empirical constant of 5 cal/mol/Å².³⁰ The compounds proposed for synthesis were among the highest scoring compounds using the most sophisticated energy function.

CHEMISTRY

As outlined in Scheme 1, activated mixed carbonates 7a–j of cyclic and acyclic alcohols used in the synthesis of designed inhibitors were prepared following the literature procedure.¹⁹ It is to be noted that attempts to use one standard activation condition was not very efficient and resulted in poor yields. Therefore, depending on the functional groups present in the P2 alcohol fragment, two different activating agents have been used. Accordingly, alcohols 6a–c,f–j were reacted with *p*-nitrophenylchloroformate and *N*-methylmorpholine in THF at 25 °C to provide corresponding carbonates 7a–c,f–j in 58–79% yields. Alcohols 6d–e were converted to corresponding succinimidyl carbonates 7d–e by treatment with *N,N'*-succinimidyl carbonate and triethylamine in acetonitrile in 35–41% isolated yields.

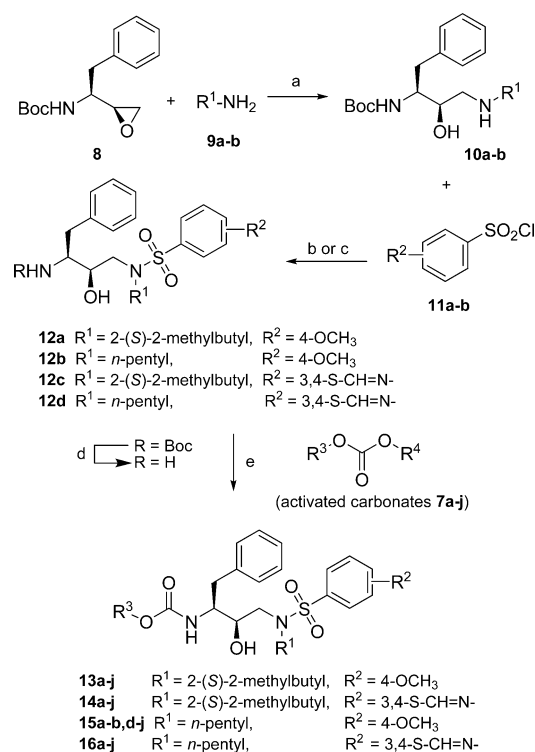
The synthesis of (*R*)-(hydroxyethylamino)sulfonamide isosteres 12 was carried out following the reported methods^{21,23} as outlined in Scheme 2. Regioselective ring-opening of commercially available epoxide 8, (1*S*,2*S*)-(1-oxiran-2-phenylethyl)carbamic acid *tert*-butyl ester, with two primary amines, (*S*)-2-methylbutylamine and *n*-pentylamine, in ethanol

Scheme 1. Synthesis of Activated Carbonate Intermediates 7a–j^a



^aReagents and conditions: (a) *N*-methylmorpholine, *p*-nitrophenylchloroformate, 0 °C to rt, 1 h; (b) *N,N'*-succinimidyl carbonate, Et₃N, CH₃CN, 0 °C to rt, 8 h.

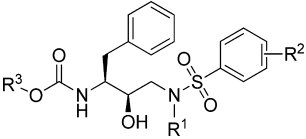
Scheme 2. Synthesis of Designed Protease Inhibitors 13a–j to 16a–j^a



^aReagents and conditions: (a) EtOH, 80 °C, 3 h; (b) aq Na₂CO₃, CH₂Cl₂, 0 °C to rt, 6 h; (c) Et₃N, CH₂Cl₂, 0 °C to rt, 5 h; (d) TFA, CH₂Cl₂, rt, 1 h; (e) Et₃N, THF, 0 °C to rt, 4–8 h.

provided β-amino alcohols 10a and 10b, respectively. Depending upon the chemical properties of selected sulfonyl chlorides,

Table 1. Inhibitory Activities of Compounds against Wild-type HIV-1 Protease



Compd	R ¹	R ²	R ³	K_i (nM) Wt/Q7K	Compd	R ¹	R ²	R ³	K_i (nM) Wt/Q7K
12b		3,4-S- CH=N-		0.243	14j		3,4-S- CH=N-		0.003
13a		4-OCH ₃		0.873	15a		4-OCH ₃		17.24
13b		4-OCH ₃		11.95	15b		4-OCH ₃		31.44
13c		4-OCH ₃		0.003	15d		4-OCH ₃		6.98
13d		4-OCH ₃		0.426	15e		4-OCH ₃		2.955
13e		4-OCH ₃		2.01	15f		4-OCH ₃		0.406
13f		4-OCH ₃		0.028	15g		4-OCH ₃		0.398
13g		4-OCH ₃		0.048	15h		4-OCH ₃		0.008
13h		4-OCH ₃		0.003	15i		4-OCH ₃		65.89
13i		4-OCH ₃		35.11	15j		4-OCH ₃		0.624
13j		4-OCH ₃		0.055	16a		3,4-S- CH=N-		11.39
14a		3,4-S- CH=N-		0.590	16b		3,4-S- CH=N-		19.67
14b		3,4-S- CH=N-		9.13	16c		3,4-S- CH=N-		0.001
14c		3,4-S- CH=N-		0.060	16d		3,4-S- CH=N-		3.375
14d		3,4-S- CH=N-		0.303	16e		3,4-S- CH=N-		1.29
14e		3,4-S- CH=N-		0.230	16f		3,4-S- CH=N-		3.345
14f		3,4-S- CH=N-		1.392	16g		3,4-S- CH=N-		0.217
14g		3,4-S- CH=N-		0.005	16h		3,4-S- CH=N-		0.017
14h		3,4-S- CH=N-		0.005	16i		3,4-S- CH=N-		42.11
14i		3,4-S- CH=N-		121.5	16j		3,4-S- CH=N-		0.027
APV				0.007	DRV				0.0002

two different methods were used for the synthesis of (*R*)-(hydroxyethylamino)sulfonamide intermediates **12a–d**. Reactions of the amino alcohols **10a,b** with *p*-(methoxy)-phenylsulfonyl chloride **11a** were carried out using aqueous sodium carbonate (Na₂CO₃) and 6-benzothiazolesulfonyl chloride **11b**, using diisopropylethylamine in anhydrous CH₂Cl₂, and furnished the corresponding sulfonamides **12a–d**. Subsequent removal of the Boc protection using trifluoroacetic acid in CH₂Cl₂ furnished the corresponding free amino alcohols. Selective alkoxy carbonylation of the aliphatic amines in amino alcohols **12a–d** using either activated *p*-nitrophenyl carbonate or succinimidyl carbonate **7a–j** of selected alcohols

under basic conditions provided the desired inhibitors **13a–j** to **16a–j** in 49–81% yields (Scheme 2).

RESULTS AND DISCUSSION

We used computational structure-based design combined with substrate-envelope constraints to design a series of novel HIV-1 PIs. The designed PIs incorporate various alcohol-derived P2 carbamates with acyclic and cyclic heteroatomic functionalities into the (*R*)-hydroxyethylamine isostere to enhance the ligand–receptor interactions in the S2 binding pocket of the protease. The (*S*)-2-methylbutyl and *n*-pentyl groups were used as P1' ligands in combination with 4-methoxyphenyl and 6-

benzothiazole groups as P2' ligands. Inhibitory activities of new PIs were determined against wild-type HIV-1 protease (Q7K) using a fluorescence resonance energy transfer (FRET) method³⁴ in a semi-high-throughput format. Chemical structures of all new inhibitors along with their inhibitory activities (K_i) are presented in Table 1; each K_i value denotes the mean of at least three independent determinations.

As predicted, introduction of cyclic and acyclic P2 carbamates with multiple hydrogen bond donor and acceptor parts provided a series of highly potent HIV-1 PIs. Compounds **13–16c**, **13–16g**, **13–16h**, and **13–16j**, containing 2,2-dichloroacetamide, imidazolidinone, oxazolidinone, and pyrrolidinone moieties, respectively, and an extended carbon chain at P2, were highly potent against wild-type protease with K_i in the low nanomolar (nM) to low picomolar (pM) range. In particular, compounds **13c** and **16c** showed impressive protease inhibitory activities with K_i of 0.003 and 0.001 nM, respectively, which are comparable to that of structurally related drugs **1** and **2**. Inhibitors **13–15h** with an oxazolidinone substituent at P2 also displayed highly potent inhibitory activities against wild-type HIV-1 protease (K_i of 0.003, 0.005, and 0.008 nM, respectively). Similarly, inhibitors **14g** and **14j** with imidazolidinone and pyrrolidinone moieties, respectively, also showed highly potent inhibitory activities. Conversely, introduction of trifluoromethylacetamide, (R)-5-hexan-2-one, and dihydrofuranone groups at the P2 carbamate in **13–16b**, **13–16d**, and **13–16i** resulted in weak inhibitory activity. Among the inhibitors **13–16a** and **13–16f** containing carbamates of (R)-methyl 3-hydroxybutanoate and its positional isomer (R)-methyl 3-hydroxy-2-methylpropanoate, respectively, only compounds **13–16f** showed better enzyme inhibitory potency. The same trend was observed for compounds **13–16e** which incorporate bis-carbamate P2 substituent. These SAR data suggest that flexible heterocyclic moieties are preferred at P2.

A subset of compounds with high binding affinity against wild-type protease was further tested against three MDR protease variants. These MDR variants were selected by examining the Stanford HIV-1 Drug Resistance Database (<http://hivdb.stanford.edu>), which contains sequences of viral isolates from HIV-1-infected patients. The selected MDR variants (L10I, G48V, I54V, L63P, V82A for M1; L10I, L63P, A71V, G73S, I84V, L90M for M2; I50V, A71V for M3) represent the pattern of resistance mutations observed under the selective pressure of three or more currently prescribed PIs.³⁵ The K_i values of selected inhibitors are presented in Table 2 with drugs **1** and **2** used as control. Most of the PIs in the current series retained high affinity against the three mutant variants (M1–M3), consistent with their wild-type protease inhibitory activities. Importantly, compounds **13c**, **13f**, **13j**, and **14j** exhibited excellent potencies in the low nanomolar ranges against all three MDR protease variants. In particular, compound **14j** with K_i of 0.003 nM against wild-type HIV-1 protease exhibited consistently higher potencies against all three MDR variants (MDR K_i of 0.240–0.377 nM).

Selected PIs were further examined for antiviral potency in cellular assays against patient derived wild-type viruses from HIV-1 clades A, B, C and two MDR HIV-1 variants; drugs **1** and **2** were used as controls (Table 3). Most of the tested compounds exhibited significant antiviral potencies with the EC_{50} values in the low nanomolar range against both wild-type and drug-resistant HIV-1 strains. Among these, three close analogues **13f**, **13j**, and **14g** exhibited modest antiviral potency. Compound **16c** with the most potent protease binding affinity

Table 2. Inhibitory Activities of Compounds against MDR Variants of HIV-1 Protease^a

compd	K_i (nM)			
	Wt	M1	M2	M3
13a	0.873	4.725	17.32	4.503
13c	0.003	0.400	0.563	0.044
13f	0.028	0.301	0.372	0.297
13g	0.048	1.974	3.256	1.056
13h	0.003	0.750	1.056	0.333
13j	0.055	0.284	0.540	0.770
14a	0.590	11.72	12.04	24.19
14c	0.060	1.481	1.269	0.265
14d	0.303	4.228	13.37	3.238
14e	0.230	3.986	3.198	2.547
14g	0.005	0.599	1.367	0.328
14i	121.5	375.2	453.1	305.7
14j	0.003	0.299	0.240	0.377
15f	0.406	2.801	1.665	1.795
16a	11.39	180.0	45.92	119.6
16c	0.001	1.345	1.074	0.057
16j	0.027	7.020	1.126	1.009
APV	0.007	0.041	0.195	0.030
DRV	0.0002	0.004	0.027	0.001

^aWt: Q7K; M1: L10I, G48V, I54V, L63P, V82A; M2: L10I, L63P, A71V, G73S, I84V, L90M; M3: I50V, A71V.

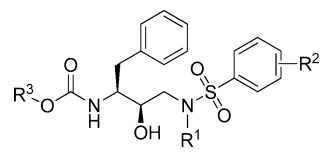
showed lower activity in cellular assays against both wild-type and MDR HIV-1 variants. Interestingly, compound **14j** with a cyclic pyrrolidinone group at the P2 position and 6-benzothiazolesulfonamide at the P2' position was the most potent against all the viruses tested (EC_{50} of 15.5–35.6 nM).

In general, inhibitors with a flexible heterocyclic moiety at P2 were considerably more potent than their inflexible and acyclic counterparts in both enzyme inhibitory and antiviral assays. These results revealed the compatibility of most of the selected P2 substituents with established P1' and P2' substituents. Thus, further optimization of these potent compounds may lead to the development of novel HIV-1 protease inhibitors active against drug-resistant HIV-1.

Crystal Structures of HIV-1 Protease Complexes.

Crystal structures of four potent inhibitors **13c**, **13f**, **13g**, and **14j** have been determined in complex with wild-type HIV-1 protease. The R³ group in the **13c**–protease complex was disordered, and the R¹ and R² groups have similar interactions as in **13f** and **13g**; hence, this structure is not discussed in detail. The backbone atoms of the protease in the three structures **13f**, **13g** and **14j** superpose well within 2.12–2.59 Å. The scaffold of the inhibitors and the R¹ and R² groups also superpose well onto each other. The conformation of the protease, including the orientations of the side chains, is similar in the regions where the three inhibitors superpose well onto each other. Both the benzothiazole and the 4-methoxyphenyl R² substituents in the three structures form hydrogen bonding interactions with the backbone amide NH of the Asp30 residue as predicted computationally and previously observed (Figure 2).

The R³ groups of **13f**, **13g**, and **14j** make different contacts in each case, providing interesting structural basis for their distinct enzymatic activities. Compound **13f** contains a methyl ester at R³ which forms a bifurcated hydrogen bond with the backbone amide NHs of Asp29 and Asp30 through its carbonyl oxygen (see Figure 2a). The methyl group of the ester packs within the

Table 3. Antiviral Activity of Protease Inhibitors against Wild-Type and MDR HIV-1 Strains^a


Compd	R ¹	R ²	R ³	EC ₅₀ (nM)					
				WT	WT-A	WT-B	WT-C	MDR	MDR1
13c		4-OCH ₃		39.1	51.3	30.7	84.6	158.7	123.0
13f		4-OCH ₃		30.9	24.9	20.6	36.3	56.0	41.8
13g		4-OCH ₃		84.4	95.4	57.3	134.8	132.1	113.3
13h		4-OCH ₃		40.5	43.3	27.8	57.3	74.4	56.1
13j		4-OCH ₃		43.9	64.5	38.5	44.1	72.2	37.1
14c		3,4-S-CH=N-		43.0	64.1	28.6	88.0	189.3	143.9
14e		3,4-S-CH=N-		197.6	231.1	183.2	331.3	917.9	755.9
14g		3,4-S-CH=N-		34.8	31.4	21.6	49.3	88.1	50.4
14h		3,4-S-CH=N-		33.3	21.2	12.0	36.2	73.6	32.2
14j		3,4-S-CH=N-		15.5	25.1	16.4	13.2	35.6	21.1
15h		4-OCH ₃		77.1	126.4	52.4	158.2	265.4	299.7
16c		3,4-S-CH=N-		38.3	79.2	30.3	67.0	285.1	253.9
16g		3,4-S-CH=N-		83.8	99.7	53.9	129.8	274.5	236.8
16h		3,4-S-CH=N-		73.0	96.3	41.1	120.5	420.0	259.4
16j		3,4-S-CH=N-		58.9	82.7	44.8	96.5	174.2	129.6
APV				3.0	2.6	1.8	3.7	17.5	15.6
DRV				0.25	0.3	0.15	0.18	0.6	0.23

^aAntiviral assays were carried out by Monogram Biosciences: WT, wild-type HIV-1 control; WT-A, WT-B, WT-C, patient-derived strains of wild-type HIV-1 from clades A, B, and C, respectively; MDR, drug-resistant HIV-1 control MDRC4; MDR1, drug-resistant HIV-1 variant with protease mutations M46I, I54V, V82A, and L90M.

hydrophobic P2 pocket containing residues Val32, Ile47, and Ile84. The side chains of Val32 and Ile84 in **13f** adopt a different conformation compared to **13g** and **14j** structures, probably to accommodate the methyl group, while the backbone of the protease is similar in all the structures. The ester oxygen atom of **13f** does not make a hydrogen bond, and thus, it would be interesting to test the corresponding keto compound. Compound **13g** contains a cyclic urea at R³ in which the carbonyl group forms two hydrogen bonds, one with the backbone amide NH of Asp29 and one with a structural water molecule held in place by the backbone carbonyl of Gly27 as shown in Figure 2b. The nitrogen NH of the urea appears to be less important. Compound **14j** contains a pyrrolidone in which the carbonyl group also forms hydrogen bonds with the backbone amide NH of Asp29 and with the structural water molecule held by Gly27. This structural water could be considered in future design efforts. In addition, the pyrrolidinone NH forms bridging hydrogen bond interactions

through a water molecule to the backbone amide NH of Asp30. Overall, the three picomolar inhibitors **13f**, **13g**, and **14j** appear to lock in the active site by forming hydrogen bonds to both sides of the floor of the active site at Asp29 and/or Asp30, which was also observed for other picomolar inhibitors from previous studies.³⁶

HIV-1 protease is highly plastic and adapts to the conformation of the inhibitor to which it binds. The conformation of the protease in all three structures is similar except for minor differences in the side chains where the R³ groups of the inhibitors are different and have different conformations. The number of hydrogen bonds is similar in all the three inhibitor complexes. The binding affinities of the three inhibitors cannot be explained by the number of hydrogen bonds alone, emphasizing that the binding affinity is a product of both enthalpic interactions (both hydrophilic and hydrophobic) and the entropy of binding.^{37,38}

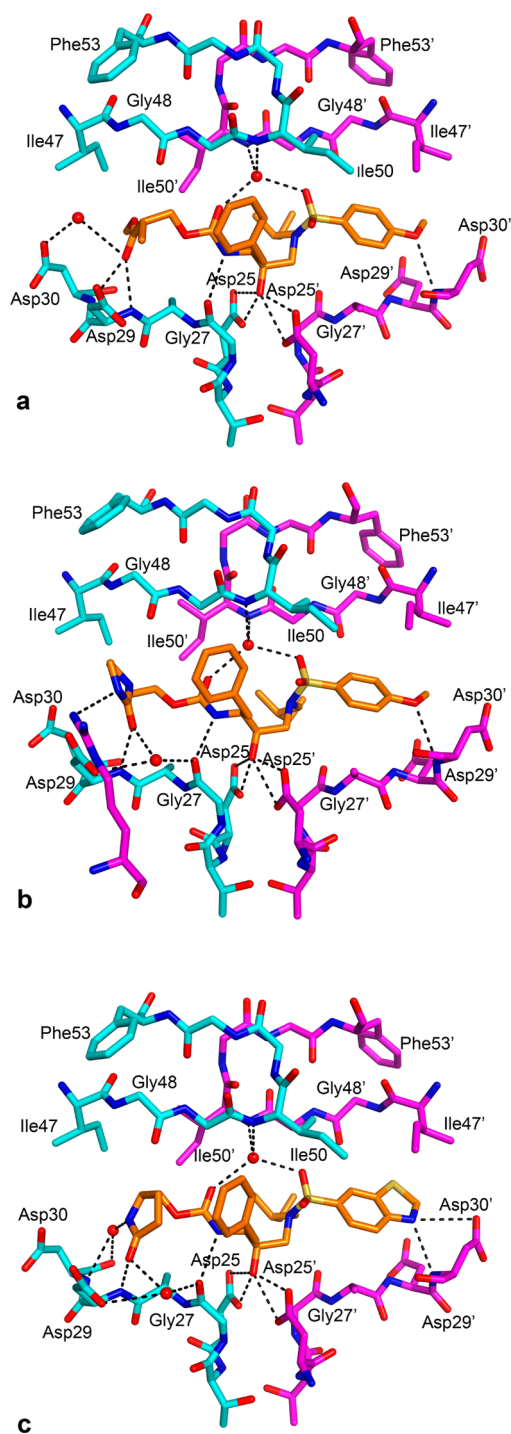


Figure 2. Hydrogen bond interactions between the wild-type protease and inhibitors in complexes of (a) **13f**, (b) **13g**, and (c) **14j**. The two monomers of the protease and the inhibitor are shown in cyan, magenta, and orange, respectively. Nitrogen, oxygen, and sulfur atoms are in blue, red, and yellow, respectively.

CONCLUSIONS

In summary, we have described a series of highly potent HIV-1 PIs based on the (hydroxyethylamino)sulfonamide isostere that incorporate various P2 carbamates of acyclic and cyclic alcohols. A number of analogues possessing the (*R*)-2-methylpropanoate, (*S*)-5-(methyl)pyrrolidin-2-one, ethyloxazolidin-2-one, and ethylimidazolidin-2-one at the P2 exhibited excellent binding affinities against wild-type HIV-1 protease and

a panel of three MDR variants. In general, PIs incorporating the flexible cyclic P2 moieties with multiple polar atoms showed highly potent inhibitory activities against wild-type protease and MDR variants. Moreover, several compounds exhibited antiviral activities with EC_{50} values in the nanomolar range. Notably, inhibitor **14j** with the (*S*)-5-(methyl)pyrrolidin-2-one P2 moiety consistently exhibited potent activity in both enzymatic and cellular assays. The X-ray crystal structure analysis of **14j** bound to HIV-1 protease revealed enhanced backbone interactions with the protease enzyme. The carbonyl oxygen and NH of the pyrrolidone P2 ligand are involved in direct and water-mediated hydrogen bonding interactions with the backbone NHs of Asp29 and Asp30 in the S2 subsite. These extensive interactions of **14j** may be responsible for its impressive activity against MDR protease variants and for its antiviral potency in cellular assays. The results from the current study support the compatibility of many selected P2 ligands, and the structure–activity relationship data can be utilized to design new protease inhibitors with better enzyme inhibitory and antiviral potencies.

EXPERIMENTAL SECTION

General. Thin-layer chromatography (TLC) was performed on silica gel (60 F-254) coated plates (Merck KGA), and spots were visualized with UV light. Flash column chromatography was performed using silica gel (230–400 mesh, Merck KGA). Proton and carbon nuclear magnetic resonance (^1H NMR and ^{13}C NMR) spectra were normally carried out in CDCl_3 solutions on a JEOL JNM-ECS spectrometer, operating at 400 MHz for ^1H NMR and 100 MHz for ^{13}C NMR. Trimethylsilane (TMS) was used as an internal standard. Chemical shifts are given in ppm relative to the trimethylsilane (TMS) solvent signal, and coupling constant (J) values are reported in hertz (Hz). Low-resolution mass spectra (ESI) were obtained using Waters Micromass model ZQ 4000 using methanol solvent. Tetrahydrofuran (THF) was distilled from sodium/benzophenone. Anhydrous dichloromethane, benzene, toluene, and *N,N*-dimethylformamide (DMF) and all other solvents and reagents were purchased from commercial vendors and were used as received. Analytical reversed-phase high performance liquid chromatography (HPLC) was performed on a Waters separation module 2695 system equipped with an autosampler and a Waters 996 photodiode array detector. Purity of the final compounds was determined using the chromatographic system parameters: column, YMC-Pack Pro C18 (particle size = 5 μm , pore size = 12 nm, dimensions = 150 mm \times 4.6 mm); mobile phase A, water; mobile phase B, methanol. By use of a flow rate of 1.0 mL/min, gradient elution was performed from 20% B to 100% B over 10 min. In every case, 10 μL of a 1 mM solution was injected. Purity data and the corresponding retention times of all final compounds have been presented in the Supporting Information.

(*R*)-Methyl 3-(((2*S*,3*R*)-3-Hydroxy-4-(4-methoxy-*N*-((*S*)-2-methylbutyl)phenylsulfonamido)-1-phenylbutan-2-yl)carbamoyloxy)butanoate (13a**).** To a solution of the *tert*-butyl ((2*S*,3*R*)-3-hydroxy-4-(4-methoxy-*N*-((*S*)-2-methylbutyl)phenylsulfonamido)-1-phenylbutan-2-yl)carbamate **12a** (0.20 g, 0.384 mmol) in CH_2Cl_2 (7 mL) was added trifluoroacetic acid (2 mL), and the resulting mixture was stirred at room temperature for 1.5 h. After completion of reaction, the reaction mixture was concentrated under reduced pressure, and the residue was dissolved in toluene (10 mL) and again evaporated under reduced pressure to dryness. The resulting deprotected amine product was dissolved in dry THF (6 mL), and the solution was cooled to 0 $^\circ\text{C}$. Diisopropylethylamine (0.2 mL, 1.21 mmol) was added, and after 10 min the activated carbonate **7a** solution in dry THF was slowly added. The resulting reaction mixture was stirred at 0 $^\circ\text{C}$ for 4 h, allowed to warm to room temperature, and stirred until reaction was complete. Water (5 mL) and EtOAc (20 mL) were added, and layers were separated; the organic layer was washed with saturated aqueous NaCl solution (10 mL), dried (Na_2SO_4),

filtered, and concentrated. The residue was purified by flash chromatography on silica gel, eluting with a mixture of 1:3 EtOAc/hexane to afford the target compound **13a** (0.17 g, 81%) as a colorless semisolid. $^1\text{H NMR}$ (400 MHz, CDCl_3) δ 7.68–7.62 (m, 2H), 7.25–7.13 (m, 5H), 6.94–6.88 (m, 2H), 5.87 (d, J = 8.5 Hz, 1H), 5.19–5.10 (m, 1H), 4.13–4.03 (m, 2H), 3.84–3.74 (m, 4H), 3.61 (s, 3H), 3.05 (dd, J = 14.9, 4.3 Hz, 1H), 2.99 (d, J = 8.5 Hz, 1H), 2.97–2.86 (m, 2H), 2.75 (dd, J = 13.4, 7.3 Hz, 1H), 2.58–2.51 (m, 1H), 2.51–2.44 (m, 1H), 2.43–2.37 (m, 1H), 2.36–2.30 (m, 1H), 2.29–2.19 (m, 1H), 1.15 (d, J = 4.8 Hz, 3H), 1.01–0.96 (m, 1H), 0.82–0.73 (m, 6H); $^{13}\text{C NMR}$ (100 MHz, CDCl_3) δ 170.67, 162.97, 155.71, 137.49, 129.75, 129.53 (2C), 129.45 (2C), 128.47 (2C), 126.46, 114.30 (2C), 72.32, 67.97, 57.33, 55.58, 54.84, 53.62, 51.63, 40.72, 35.47, 33.39, 26.35, 20.07, 16.84, 11.00; MS (ESI) m/z 587.16 (M + Na) $^+$.

2-(2,2-Trifluoroacetamido)ethyl ((2S,3R)-3-Hydroxy-4-(4-methoxy-*N*-((S)-2-methylbutyl)phenylsulfonamido)-1-phenylbutan-2-yl)carbamate (13b). The title compound was obtained from **12a** and **7b** as described for **13a** in 71% yield after flash chromatography (1:4 EtOAc/hexane) as an amorphous white solid. $^1\text{H NMR}$ (400 MHz, CDCl_3) δ 7.82 (d, J = 8.5 Hz, 1H), 7.66–7.59 (m, 2H), 7.23–7.11 (m, 5H), 6.92–6.87 (m, 2H), 4.29 (t, J = 7.8 Hz, 1H), 4.11–3.97 (m, 1H), 3.86–3.83 (m, 1H), 3.81–3.74 (m, 4H), 3.57–3.41 (m, 1H), 3.13 (dd, J = 15.2, 9.2 Hz, 1H), 3.05–2.79 (m, 4H), 2.73–2.67 (m, 1H), 2.44–2.31 (m, 1H), 1.75 (bs, 1H), 1.57–1.48 (m, 1H), 1.44–1.35 (m, 1H), 1.20–1.14 (m, 1H), 1.04–0.92 (m, 1H), 0.85–0.72 (m, 6H); $^{13}\text{C NMR}$ (100 MHz, CDCl_3) δ 162.95, 155.42, 151.56, 137.28, 129.43, 129.36 (2C), 129.24 (2C), 128.42 (2C), 128.39, 126.53, 114.28 (2C), 72.26, 62.25, 55.53, 54.73, 53.21, 42.30, 35.86, 33.33, 29.62, 26.39, 16.84, 10.94; MS (ESI) m/z 626.31 (M + Na) $^+$.

2-(2,2-Dichloroacetamido)ethyl ((2S,3R)-3-Hydroxy-4-(4-methoxy-*N*-((S)-2-methylbutyl)phenylsulfonamido)-1-phenylbutan-2-yl)carbamate (13c). The title compound was obtained from **12a** and **7c** as described for **13a** in 57% yield after flash chromatography (1:4 EtOAc/hexane) as a colorless viscous liquid. $^1\text{H NMR}$ (400 MHz, CDCl_3) δ 7.63 (d, J = 9.2 Hz, 2H), 7.24–7.09 (m, 5H), 6.99 (bs, 1H), 6.91 (d, J = 8.5 Hz, 2H), 5.89 (s, 1H), 5.04 (d, J = 9.2 Hz, 1H), 4.09–3.97 (m, 2H), 3.86–3.76 (m, 5H), 3.74–3.56 (m, 2H), 3.47–3.33 (m, 2H), 3.14–2.67 (m, 5H), 1.67–1.46 (m, 2H), 1.05–0.95 (m, 1H), 0.83–0.70 (m, 6H); $^{13}\text{C NMR}$ (100 MHz, CDCl_3) δ 164.30, 163.05, 156.36, 137.46, 129.63 (2C), 129.42 (2C), 128.84 (2C), 128.48, 126.58, 114.33 (2C), 72.24, 66.22, 63.01, 57.13, 55.60, 55.07, 53.35, 40.28, 35.34, 33.34, 26.41, 16.86, 11.00; MS (ESI) m/z 640.19 (M – 1 + Na) $^+$, 642.19 (M + 1 + Na) $^+$.

(R)-5-Oxohexan-2-yl ((2S,3R)-3-Hydroxy-4-(4-methoxy-*N*-((S)-2-methylbutyl)phenylsulfonamido)-1-phenylbutan-2-yl)carbamate (13d). The title compound was obtained from **12a** and **7d** as described for **13a** in 69% yield after flash chromatography (1:3 EtOAc/hexane) as an amorphous white solid. $^1\text{H NMR}$ (400 MHz, CDCl_3) δ 7.66–7.60 (m, 2H), 7.25–7.10 (m, 5H), 6.95–6.86 (m, 2H), 4.69 (d, J = 7.9 Hz, 1H), 4.63–4.54 (m, 1H), 3.88–3.67 (m, 6H), 3.10–2.89 (m, 4H), 2.89–2.67 (m, 2H), 2.35 (t, J = 6.7 Hz, 1H), 2.02 (s, 3H), 1.79–1.50 (m, 4H), 1.47–1.36 (m, 1H), 1.09–0.93 (m, 4H), 0.84–0.72 (m, 6H); $^{13}\text{C NMR}$ (100 MHz, CDCl_3) δ 207.90, 163.00, 156.21, 137.63, 129.78, 129.44 (4C), 128.47 (2C), 126.47, 114.31 (2C), 79.35, 72.36, 70.93, 57.23, 55.60, 54.88, 53.50, 39.47, 35.27, 33.39, 29.88, 26.40, 20.18, 16.88, 11.01; MS (ESI) m/z 585.40 (M + Na) $^+$.

2-((tert-Butoxycarbonyl)amino)ethyl ((2S,3R)-3-Hydroxy-4-(4-methoxy-*N*-((S)-2-methylbutyl)phenylsulfonamido)-1-phenylbutan-2-yl)carbamate (13e). The title compound was obtained from **12a** and **7e** as described for **13a** in 51% yield after flash chromatography (1:3 EtOAc/hexane) as an amorphous white solid. $^1\text{H NMR}$ (400 MHz, CDCl_3) δ 7.66 (d, J = 8.5 Hz, 2H), 7.30–7.12 (m, 5H), 6.93 (d, J = 7.9 Hz, 2H), 5.15–4.92 (m, 1H), 4.80 (bs, 1H), 4.01–3.88 (m, 2H), 3.85–3.73 (m, 5H), 3.65–3.61 (m, 1H), 3.43–3.29 (m, 1H), 3.28–3.15 (m, 3H), 3.08–2.91 (m, 4H), 1.58–1.44 (m, 1H), 1.43–1.28 (m, 10H), 1.03–0.93 (m, 1H), 0.85–0.69 (m, 6H); $^{13}\text{C NMR}$ (100 MHz, CDCl_3) δ 162.96, 156.45, 155.81, 137.63, 131.01, 129.72 (2C), 129.40 (2C), 128.41 (2C), 126.46, 114.26 (2C),

79.51, 72.27, 62.36, 57.09, 55.54, 53.34, 43.03, 41.96, 35.27, 33.30, 28.30 (3C), 26.40, 16.83, 10.96; MS (ESI) m/z 630.52 (M + Na) $^+$.

(R)-Methyl 3-(((2S,3R)-3-Hydroxy-4-(4-methoxy-*N*-((S)-2-methylbutyl)phenylsulfonamido)-1-phenylbutan-2-yl)-carbamoyloxy)-2-methylpropanoate (13f). The title compound was obtained from **12a** and **7f** as described for **13a** in 63% yield after flash chromatography (1:3 EtOAc/hexane) as an amorphous white solid. $^1\text{H NMR}$ (400 MHz, CDCl_3) δ 7.64–7.60 (m, 2H), 7.25–7.11 (m, 5H), 6.92–6.88 (m, 2H), 4.82–4.79 (m, 1H), 4.08–3.97 (m, 2H), 3.80 (s, 3H), 3.77–3.60 (m, 3H), 3.57 (s, 3H), 3.07–2.79 (m, 5H), 2.75–2.58 (m, 2H), 1.58–1.35 (m, 2H), 1.04 (d, J = 6.7 Hz, 3H), 1.02–0.93 (m, 1H), 0.83–0.72 (m, 6H); $^{13}\text{C NMR}$ (100 MHz, CDCl_3) δ 174.23, 162.96, 156.05, 137.43, 129.70, 129.46 (2C), 129.43 (2C), 128.46 (2C), 126.56, 114.26 (2C), 72.27, 65.96, 57.26, 55.56, 54.92, 53.57, 51.79, 39.23, 35.36, 33.36, 26.33, 16.82, 13.51, 10.95; MS (ESI) m/z 587.35 (M + Na) $^+$.

2-(2-Oxoimidazolidin-1-yl)ethyl ((2S,3R)-3-Hydroxy-4-(4-methoxy-*N*-((S)-2-methylbutyl)phenylsulfonamido)-1-phenylbutan-2-yl)carbamate (13g). The title compound was obtained from **12a** and **7g** as described for **13a** in 51% yield after flash chromatography (1:4 EtOAc/hexane) as an amorphous white solid. $^1\text{H NMR}$ (400 MHz, CDCl_3) δ 7.64 (d, J = 8.5 Hz, 2H), 7.23–7.07 (m, 5H), 6.89 (d, J = 8.5 Hz, 2H), 5.30 (m, 1H), 5.00 (bs, 1H), 4.17–3.97 (m, 2H), 3.96–3.88 (m, 1H), 3.87–3.79 (m, 2H), 3.78 (s, 3H), 3.35–3.16 (m, 6H), 3.06–2.97 (m, 2H), 2.96–2.84 (m, 2H), 2.83–2.69 (m, 2H), 1.63–1.48 (m, 1H), 1.41–1.26 (m, 1H), 1.05–0.85 (m, 1H), 0.81–0.70 (m, 6H); $^{13}\text{C NMR}$ (100 MHz, CDCl_3) δ 162.80, 162.75, 155.98, 137.86, 129.97, 129.38 (2C), 129.27 (2C), 128.28 (2C), 126.24, 114.15 (2C), 72.04, 62.10, 56.76, 55.50, 55.00, 52.96, 45.25, 42.80, 38.09, 34.98, 33.18, 26.46, 16.79, 10.96; MS (ESI) m/z 599.32 (M + Na) $^+$.

2-(2-Oxooxazolidin-3-yl)ethyl ((2S,3R)-3-Hydroxy-4-(4-methoxy-*N*-((S)-2-methylbutyl)phenylsulfonamido)-1-phenylbutan-2-yl)carbamate (13h). The title compound was obtained from **12a** and **7h** as described for **13a** in 68% yield after flash chromatography (1:3 EtOAc/hexane) as a colorless viscous liquid. $^1\text{H NMR}$ (400 MHz, CDCl_3) δ 7.69–7.67 (m, 2H), 7.25–7.14 (m, 5H), 6.95–6.63 (m, 2H), 5.05 (d, J = 7.9 Hz, 1H), 4.34–3.99 (m, 4H), 3.93–3.66 (m, 6H), 3.48–3.27 (m, 4H), 3.14–2.92 (m, 4H), 2.91–2.73 (m, 2H), 2.68–2.50 (m, 1H), 1.51–1.34 (m, 1H), 1.13–0.91 (m, 1H), 0.94–0.74 (m, 6H); $^{13}\text{C NMR}$ (100 MHz, CDCl_3) δ 162.90, 158.51, 155.83, 137.64, 129.86, 129.38 (2C), 129.32 (2C), 128.36 (2C), 126.35, 114.23 (2C), 72.06, 61.82, 57.02, 55.55, 55.00, 53.16, 44.81, 43.60, 35.21, 33.28, 26.38, 20.92, 16.78, 10.96; MS (ESI) m/z 599.86 (M + Na) $^+$.

(R)-2-Oxotetrahydrofuran-3-yl ((2S,3R)-3-Hydroxy-4-(4-methoxy-*N*-((S)-2-methylbutyl)phenylsulfonamido)-1-phenylbutan-2-yl)carbamate (13i). The title compound was obtained from **12a** and **7i** as described for **13a** in 64% yield after flash chromatography (1:3 EtOAc/hexane) as a colorless viscous liquid. $^1\text{H NMR}$ (400 MHz, CDCl_3) δ 7.76–7.69 (m, 2H), 7.31–7.15 (m, 5H), 7.02–6.96 (m, 2H), 4.60 (t, J = 5.5 Hz, 1H), 4.33–4.21 (m, 1H), 3.87 (s, 3H), 3.84–3.76 (m, 1H), 3.75–3.56 (m, 2H), 3.38–3.14 (m, 3H), 3.13–3.01 (m, 1H), 2.99–2.80 (m, 2H), 2.10–1.96 (m, 1H), 1.95–1.65 (m, 3H), 1.63–1.51 (m, 1H), 1.50–1.36 (m, 1H), 1.13–0.97 (m, 1H), 0.91–0.78 (m, 6H); $^{13}\text{C NMR}$ (100 MHz, CDCl_3) δ 173.73, 163.05, 155.59, 136.73, 129.88, 129.59 (2C), 129.22, 129.09, 128.65 (2C), 127.00, 114.36 (2C), 76.35, 70.88, 57.21, 55.64, 52.79, 33.45, 32.90, 32.61, 32.13, 31.95, 26.64, 16.84, 10.08; MS (ESI) m/z 571.34 (M + Na) $^+$.

(S)-5-Oxopyrrolidin-2-ylmethyl ((2S,3R)-3-Hydroxy-4-(4-methoxy-*N*-((S)-2-methylbutyl)phenylsulfonamido)-1-phenylbutan-2-yl)carbamate (13j). The title compound was obtained from **12a** and **7j** as described for **13a** in 59% yield after flash chromatography (1:3 EtOAc/hexane) as an amorphous white solid. $^1\text{H NMR}$ (400 MHz, CDCl_3) δ 7.67 (d, J = 8.5 Hz, 2H), 7.32–7.11 (m, 6H), 6.92 (d, J = 8.5 Hz, 2H), 5.60 (d, J = 8.5 Hz, 1H), 4.15–3.99 (m, 2H), 3.69–3.60 (m, 7H), 3.18–2.68 (m, 4H), 2.38–2.18 (m, 2H), 2.15–2.04 (m, 1H), 1.71–1.28 (m, 4H), 1.11–0.86 (m, 2H), 0.89–0.71 (m, 6H); $^{13}\text{C NMR}$ (100 MHz, CDCl_3) δ 178.63, 162.76, 155.82,

137.84, 129.96, 129.34 (2C), 129.28 (2C), 128.24 (2C), 126.25, 114.12 (2C), 72.01, 67.20, 56.65, 55.45, 55.15, 53.20, 52.95, 34.95, 33.14, 29.64, 26.44, 22.67, 16.78, 10.92; MS (ESI) m/z 584.01 (M + Na)⁺.

(R)-Methyl 3-(((2S,3R)-3-Hydroxy-4-(N-((S)-2-methylbutyl)-benzo[d]thiazole-6-sulfonamido)-1-phenylbutan-2-yl)-carbamoyloxy)butanoate (14a). The title compound was obtained from **12b** and **7a** as described for **13a** in 46% yield after flash chromatography (1:2 EtOAc/hexane) as colorless viscous liquid. ¹H NMR (400 MHz, CDCl₃) δ 9.13 (s, 1H), 8.40 (d, J = 1.8 Hz, 1H), 8.17 (d, J = 8.5 Hz, 1H), 7.83 (dd, J = 8.5, 1.8 Hz, 1H), 7.25–7.15 (m, 5H), 6.02 (d, J = 7.9 Hz, 1H), 5.18–5.09 (m, 1H), 4.14–4.05 (m, 2H), 3.82–3.76 (m, 1H), 3.60 (s, 3H), 3.10 (dd, J = 14.9, 3.9 Hz, 1H), 3.08–3.03 (m, 1H), 3.02–2.92 (m, 1H), 2.94–2.83 (m, 2H), 2.76 (dd, J = 14.1, 7.0 Hz, 1H), 2.56–2.47 (m, 1H), 2.42–2.35 (m, 1H), 2.29–2.19 (m, 1H), 1.44–1.32 (m, 1H), 1.13 (d, J = 6.1 Hz, 3H), 1.01–0.96 (m, 1H), 0.83–0.73 (m, 6H); ¹³C NMR (100 MHz, CDCl₃) δ 172.05, 170.72, 157.89, 155.46, 137.66, 135.87, 134.26, 129.31 (2C), 128.54 (2C), 126.58, 124.84, 124.25, 122.24, 72.29, 67.57, 57.10, 54.17, 53.06, 51.78, 40.29, 35.03, 33.35, 26.47, 19.70, 16.79, 11.03; MS (ESI) m/z 614.26 (M + Na)⁺.

2-(2,2-Trifluoroacetamido)ethyl ((2S,3R)-3-Hydroxy-4-(N-((S)-2-methylbutyl)benzo[d]thiazole-6-sulfonamido)-1-phenylbutan-2-yl)carbamate (14b). The title compound was obtained from **12b** and **7b** as described for **13a** in 66% yield after flash chromatography (1:2 EtOAc/hexane) as a colorless viscous liquid. ¹H NMR (400 MHz, CDCl₃) δ 9.14 (s, 1H), 8.40 (d, J = 1.8 Hz, 1H), 8.17 (d, J = 8.5 Hz, 1H), 7.85–7.78 (m, 2H), 7.23–7.11 (m, 6H), 4.30 (t, J = 8.0 Hz, 2H), 4.07–3.99 (m, 1H), 3.88–3.78 (m, 3H), 3.56 (d, J = 3.7 Hz, 1H), 3.15 (dd, J = 15.3, 9.2 Hz, 1H), 3.06–2.94 (m, 2H), 2.89–2.78 (m, 2H), 1.57–1.49 (m, 1H), 1.44–1.36 (m, 1H), 1.06–0.94 (m, 2H), 0.87–0.70 (m, 6H); ¹³C NMR (100 MHz, CDCl₃) δ 157.94, 155.50, 155.44, 151.66, 137.35, 134.32, 132.74, 129.43 (2C), 129.23, 128.50 (2C), 126.65, 124.88, 124.31, 122.34, 71.90, 62.27, 57.03, 54.83, 53.11, 42.30, 35.95, 33.27, 26.37, 16.86, 10.98; MS (ESI) m/z 653.37 (M + Na)⁺.

2-(2,2-Dichloroacetamido)ethyl ((2S,3R)-3-Hydroxy-4-(N-((S)-2-methylbutyl)benzo[d]thiazole-6-sulfonamido)-1-phenylbutan-2-yl)carbamate (14c). The title compound was obtained from **12b** and **7c** as described for **13a** in 61% yield after flash chromatography (1:2 EtOAc/hexane) as foam. ¹H NMR (400 MHz, CDCl₃) δ 9.14 (s, 1H), 8.37 (d, J = 2.1 Hz, 1H), 8.17 (dd, J = 8.5, 2.4 Hz, 1H), 7.81 (dd, J = 8.5, 1.8 Hz, 1H), 7.31–7.08 (m, 5H), 6.98 (bs, 1H), 5.81 (s, 1H), 5.12 (bs, 1H), 5.07 (d, J = 7.9 Hz, 1H), 4.09–3.97 (m, 2H), 3.87–3.81 (m, 1H), 3.75–3.58 (m, 2H), 3.47–3.33 (m, 2H), 3.14–2.67 (m, 5H), 1.66–1.45 (m, 2H), 1.06–0.93 (m, 1H), 0.86–0.72 (m, 6H); ¹³C NMR (100 MHz, CDCl₃) δ 163.43, 157.20, 156.87, 154.57, 135.52, 135.02, 133.42, 128.50, 128.28, 127.92, 127.60, 126.48, 123.81, 123.44, 121.25, 72.24, 65.37, 63.43, 56.02, 54.80, 54.71, 47.29, 34.97, 25.91, 16.95, 14.16, 11.32; MS (ESI) m/z 666.99 (M - 1 + Na)⁺, 668.93 (M + 1 + Na)⁺.

(R)-5-Oxoheptan-2-yl ((2S,3R)-3-Hydroxy-4-(N-((S)-2-methylbutyl)benzo[d]thiazole-6-sulfonamido)-1-phenylbutan-2-yl)carbamate (14d). The title compound was obtained from **12b** and **7d** as described for **13a** in 55% yield after flash chromatography (1:2 EtOAc/hexane) as an amorphous white solid. ¹H NMR (400 MHz, CDCl₃) δ 9.14 (s, 1H), 8.39 (d, J = 1.2 Hz, 1H), 8.17 (d, J = 9.2 Hz, 1H), 7.82 (dd, J = 8.5, 1.8 Hz, 1H), 7.23–7.06 (m, 6H), 4.72 (d, J = 7.9 Hz, 1H), 4.63–4.55 (m, 1H), 3.87–3.67 (m, 3H), 3.15–2.99 (m, 3H), 2.97–2.91 (m, 1H), 2.89–2.79 (m, 1H), 2.33 (t, J = 7.3 Hz, 1H), 2.00 (s, 3H), 1.79–1.51 (m, 4H), 1.45–1.34 (m, 1H), 1.07–0.92 (m, 4H), 0.85–0.72 (m, 6H); ¹³C NMR (100 MHz, CDCl₃) δ 207.93, 157.96, 156.23, 155.47, 137.56, 135.76, 134.28, 129.40 (2C), 128.49 (2C), 126.53, 124.80, 124.30, 122.22, 72.22, 71.02, 56.98, 55.01, 53.24, 39.44, 35.20, 33.33, 29.83, 29.77, 26.39, 20.14, 16.83, 11.00; MS (ESI) m/z 612.06 (M + Na)⁺.

2-(tert-Butoxycarbonylamino)ethyl ((2S,3R)-3-Hydroxy-4-(N-((S)-2-methylbutyl)benzo[d]thiazole-6-sulfonamido)-1-phenylbutan-2-yl)carbamate (14e). The title compound was obtained from **12b** and **7e** as described for **13a** in 49% yield after flash chromatography (1:2 EtOAc/hexane) as a colorless viscous liquid. ¹H

NMR (400 MHz, CDCl₃) δ 9.14 (s, 1H), 8.38 (m, 1H), 8.14 (d, J = 8.5 Hz, 1H), 7.82 (dd, J = 8.5, 1.8 Hz, 1H), 7.24–7.11 (m, 5H), 4.86 (d, J = 6.7 Hz, 1H), 4.65 (bs, 1H), 3.98–3.88 (m, 2H), 3.86–3.74 (m, 2H), 3.70 (bs, 1H), 3.30–2.92 (m, 6H), 2.89–2.75 (m, 2H), 1.62–1.47 (m, 2H), 1.36 (s, 9H), 1.06–0.93 (m, 1H), 0.85–0.73 (m, 6H); ¹³C NMR (100 MHz, CDCl₃) δ 157.95, 156.27, 155.78, 155.56, 137.47, 135.67, 134.34, 129.47 (2C), 128.58 (2C), 126.68, 124.83, 124.38, 122.26, 79.51, 72.20, 64.36, 57.14, 55.09, 53.41, 39.95, 35.27, 33.40, 28.35 (3C), 26.41, 16.87, 11.02; MS (ESI) m/z 657.37 (M + Na)⁺.

(R)-Methyl 3-(((2S,3R)-3-Hydroxy-4-(N-((S)-2-methylbutyl)-benzo[d]thiazole-6-sulfonamido)-1-phenylbutan-2-yl)-carbamoyloxy)-2-methylpropanoate (14f). The title compound was obtained from **12b** and **7f** as described for **13a** in 68% yield after flash chromatography (1:2 EtOAc/hexane) as an amorphous white solid. ¹H NMR (400 MHz, CDCl₃) δ 9.13 (s, 1H), 8.37 (d, J = 1.2 Hz, 1H), 8.17 (d, J = 8.5 Hz, 1H), 7.82 (dd, J = 8.5, 1.8 Hz, 1H), 7.24–7.11 (m, 5H), 4.86 (d, J = 7.9 Hz, 1H), 4.08–3.97 (m, 2H), 3.82–3.68 (m, 3H), 3.56 (s, 3H), 3.14–2.92 (m, 4H), 2.89–2.72 (m, 2H), 2.69–2.57 (m, 1H), 1.62–1.47 (m, 1H), 1.46–1.36 (m, 1H), 1.06–0.96 (m, 4H), 0.82–0.70 (m, 6H); ¹³C NMR (100 MHz, CDCl₃) δ 174.21, 157.98, 156.11, 155.45, 137.36, 135.62, 134.25, 129.41 (2C), 128.49 (2C), 126.54, 124.80, 124.25, 122.20, 72.23, 66.01, 57.11, 55.05, 53.41, 51.83, 39.21, 35.35, 33.33, 26.34, 16.78, 13.48, 10.95; MS (ESI) m/z 614.30 (M + Na)⁺.

2-(2-Oxoimidazolidin-1-yl)ethyl ((2S,3R)-3-Hydroxy-4-(N-((S)-2-methylbutyl)benzo[d]thiazole-6-sulfonamido)-1-phenylbutan-2-yl)carbamate (14g). The title compound was obtained from **12b** and **7g** as described for **13a** in 57% yield after flash chromatography (1:2 EtOAc/hexane) as an amorphous white solid. ¹H NMR (400 MHz, CDCl₃) δ 9.13 (s, 1H), 8.41–8.38 (m, 1H), 8.16 (d, J = 9.2 Hz, 1H), 7.84 (dd, J = 8.5, 1.8 Hz, 1H), 7.24–7.09 (m, 6H), 5.28 (m, 1H), 4.81 (bs, 1H), 4.20–4.00 (m, 2H), 3.97–3.55 (m, 3H), 3.48–3.21 (m, 5H), 3.19–3.06 (m, 2H), 3.01–2.87 (m, 3H), 2.79–2.71 (m, 1H), 1.64–1.44 (m, 1H), 1.37–3.25 (m, 1H), 1.07–0.82 (m, 1H), 0.85–0.70 (m, 6H); ¹³C NMR (100 MHz, CDCl₃) δ 162.77, 157.93, 156.05, 155.36, 137.78, 136.03, 134.20, 129.28 (2C), 128.39 (2C), 126.39, 124.89, 124.16, 122.27, 71.76, 61.85, 56.54, 55.15, 52.71, 45.10, 42.86, 38.11, 34.89, 33.18, 26.50, 16.83, 11.03; MS (ESI) m/z 626.34 (M + Na)⁺.

2-(2-Oxooxazolidin-3-yl)ethyl ((2S,3R)-3-Hydroxy-4-(N-((S)-2-methylbutyl)benzo[d]thiazole-6-sulfonamido)-1-phenylbutan-2-yl)carbamate (14h). The title compound was obtained from **12b** and **7h** as described for **13a** in 55% yield after flash chromatography (1:2 EtOAc/hexane) as a colorless semisolid. ¹H NMR (400 MHz, CDCl₃) δ 9.12 (s, 1H), 8.46 (d, J = 1.4 Hz, 1H), 8.22 (d, J = 8.7 Hz, 1H), 7.89 (dd, J = 8.7, 1.8 Hz, 1H), 7.34–7.14 (m, 6H), 5.07 (d, J = 8.6 Hz, 1H), 4.30–4.07 (m, 3H), 4.08–3.94 (m, 1H), 3.94–3.77 (m, 1H), 3.56–3.36 (m, 3H), 3.24–3.13 (m, 2H), 3.10–3.05 (m, 1H), 3.02–2.97 (m, 2H), 2.94–2.83 (m, 2H), 1.69–1.54 (m, 1H), 1.51–1.32 (m, 1H), 1.10–0.89 (m, 1H), 0.85–0.78 (m, 6H); ¹³C NMR (100 MHz, CDCl₃) δ 158.57, 157.95, 155.90, 155.42, 137.52, 135.88, 134.24, 129.35 (2C), 128.83, 128.46, 126.48, 124.86, 124.21, 122.24, 71.78, 61.79, 56.86, 55.10, 54.72, 52.95, 44.60, 43.65, 35.15, 33.29, 26.39, 16.79, 11.01; MS (ESI) m/z 626.90 (M + Na)⁺.

(R)-2-Oxotetrahydrofuran-3-yl ((2S,3R)-3-Hydroxy-4-(N-((S)-2-methylbutyl)benzo[d]thiazole-6-sulfonamido)-1-phenylbutan-2-yl)carbamate (14i). The title compound was obtained from **12b** and **7i** as described for **13a** in 62% yield after flash chromatography (1:2 EtOAc/hexane) as a colorless viscous liquid. ¹H NMR (400 MHz, CDCl₃) δ 9.15 (s, 1H), 8.45 (d, J = 3.7 Hz, 1H), 8.18 (dd, J = 8.5, 5.5 Hz, 1H), 7.87–7.81 (m, 1H), 7.26–7.12 (m, 6H), 4.58 (d, J = 4.9 Hz, 1H), 4.50–4.36 (m, 1H), 4.36–4.23 (m, 1H), 3.85–3.56 (m, 3H), 3.37–3.07 (m, 3H), 3.05–2.91 (m, 2H), 1.61 (bs, 1H), 1.50–1.33 (m, 2H), 1.27–1.19 (m, 1H), 1.12–0.96 (m, 2H), 0.87–0.73 (m, 6H); ¹³C NMR (100 MHz, CDCl₃) δ 173.72, 158.10, 155.55, 155.46, 136.59, 135.82, 134.31, 129.06 (2C), 128.65 (2C), 127.03, 124.88, 124.30, 122.43, 76.34, 70.77, 57.04, 52.66, 33.37, 32.50, 32.17, 29.66, 28.68, 26.58, 16.79, 11.05; MS (ESI) m/z 598.32 (M + Na)⁺.

(S)-5-Oxopyrrolidin-2-ylmethyl ((2S,3R)-3-Hydroxy-4-(N-((S)-2-methylbutyl)benzo[d]thiazole-6-sulfonamido)-1-phenylbutan-2-yl)carbamate (14j). The title compound was obtained from 12b and 7j as described for 13a in 60% yield after flash chromatography (1:2 EtOAc/hexane) as a white solid. ^1H NMR (400 MHz, CDCl_3) δ 9.12 (s, 1H), 8.39 (s, 1H), 8.14 (d, $J = 8.5$ Hz, 1H), 7.82 (d, $J = 8.5$ Hz, 1H), 7.24–7.09 (m, 6H), 5.62 (d, $J = 9.2$ Hz, 1H), 4.16–3.94 (m, 2H), 3.93–3.51 (m, 3H), 3.24–3.03 (m, 2H), 3.01–2.83 (m, 3H), 2.81–2.69 (m, 1H), 2.33–1.98 (m, 4H), 1.69–1.42 (m, 2H), 1.39–1.26 (m, 1H), 1.06–0.89 (m, 1H), 0.80–0.69 (m, 6H); ^{13}C NMR (100 MHz, CDCl_3) δ 177.85, 156.99, 155.01, 154.27, 136.75, 134.97, 133.13, 128.92 (2C), 128.09 (2C), 125.37, 123.83, 123.04, 121.16, 71.81, 66.25, 55.37, 54.22, 52.23, 51.67, 33.86, 32.09, 28.68, 25.47, 21.82, 16.06, 10.16; MS (ESI) m/z 611.29 ($\text{M} + \text{Na}$) $^+$.

(R)-Methyl 3-(((2S,3R)-3-Hydroxy-4-(4-methoxy-N-pentylphenylsulfonamido)-1-phenylbutan-2-yl)carbamoyl)oxy)butanoate (15a). The title compound was obtained from 12c and 7a as described for 13a in 63% yield after flash chromatography (1:3 EtOAc/hexane) as an amorphous white solid. ^1H NMR (400 MHz, CDCl_3) δ 7.69–7.62 (m, 2H), 7.21–7.12 (m, 5H), 6.92–6.86 (m, 2H), 6.01 (d, $J = 8.5$ Hz, 1H), 5.20–5.12 (m, 1H), 4.16–3.97 (m, 2H), 3.86–3.76 (m, 4H), 3.60 (s, 3H), 3.20 (dd, $J = 14.6, 4.9$ Hz, 1H), 3.05–2.87 (m, 3H), 2.54–2.42 (m, 3H), 1.50–1.31 (m, 2H), 1.25–1.10 (m, 8H), 0.78 (t, $J = 6.7$ Hz, 3H); ^{13}C NMR (100 MHz, CDCl_3) δ 171.95, 167.71, 162.92, 137.87, 130.46, 129.31 (2C), 129.25 (2C), 128.49 (2C), 126.48, 114.28 (2C), 72.27, 67.57, 55.57, 54.41, 51.77, 50.41, 40.35, 35.04, 30.99, 29.62, 28.81, 21.26, 19.76, 13.93; MS (ESI) m/z 587.16 ($\text{M} + \text{Na}$) $^+$.

2-(2,2,2-trifluoroacetamido)ethyl ((2S,3R)-3-Hydroxy-4-(4-methoxy-N-pentylphenylsulfonamido)-1-phenylbutan-2-yl)carbamate (15b). The title compound was obtained from 12c and 7b as described for 13a in 56% yield after flash chromatography (1:3 EtOAc/hexane) as a colorless viscous liquid. ^1H NMR (400 MHz, CDCl_3) δ 7.81 (d, $J = 8.5$ Hz, 1H), 7.68–7.59 (m, 2H), 7.24–7.12 (m, 5H), 6.92–6.86 (m, 2H), 4.29 (t, $J = 7.9$ Hz, 1H), 4.08–3.96 (m, 1H), 3.91–3.75 (m, 5H), 3.57–3.42 (m, 1H), 3.14–3.07 (m, 1H), 3.05–2.96 (m, 2H), 2.94–2.77 (m, 3H), 2.44–2.33 (m, 1H), 1.68 (bs, 1H), 1.48–1.32 (m, 2H), 1.22–1.09 (m, 5H), 0.77 (t, $J = 7.8$ Hz, 3H); ^{13}C NMR (100 MHz, CDCl_3) δ 162.92, 155.42, 151.65, 137.39, 130.31, 129.43 (2C), 129.36 (2C), 129.24, 128.42 (2C), 126.53, 114.28 (2C), 72.00, 62.52, 55.58, 54.75, 52.13, 50.34, 42.29, 35.80, 28.69, 28.13, 22.13, 13.89; MS (ESI) m/z 626.32 ($\text{M} + \text{Na}$) $^+$.

(R)-5-Oxohexan-2-yl ((2S,3R)-3-Hydroxy-4-(4-methoxy-N-pentylphenylsulfonamido)-1-phenylbutan-2-yl)carbamate (15d). The title compound was obtained from 12c and 7d as described for 13a in 71% yield after flash chromatography (1:3 EtOAc/hexane) as an amorphous white solid. ^1H NMR (400 MHz, CDCl_3) δ 7.66–7.61 (m, 2H), 7.25–7.10 (m, 5H), 6.94–6.86 (m, 2H), 4.89–4.81 (m, 1H), 4.75 (d, $J = 7.7$ Hz, 1H), 4.64–4.56 (m, 1H), 3.92–3.67 (m, 5H), 3.18–2.99 (m, 3H), 2.98–2.92 (m, 1H), 2.89–2.79 (m, 1H), 2.36 (t, $J = 7.3$ Hz, 1H), 2.03 (s, 3H), 1.75–1.58 (m, 2H), 1.48–1.35 (m, 2H), 1.53–1.25 (m, 2H), 1.26–1.04 (m, 4H), 1.02 (d, $J = 6.1$ Hz, 3H), 0.78 (t, $J = 7.3$ Hz, 3H); ^{13}C NMR (100 MHz, CDCl_3) δ 207.96, 168.71, 162.97, 151.14, 137.74, 130.30, 129.44, 129.31 (2C), 128.44 (2C), 126.74, 114.30 (2C), 79.35, 72.27, 71.06, 55.50, 52.23, 50.40, 39.46, 38.56, 35.20, 29.86, 28.74, 25.42, 22.17, 19.81, 13.90; MS (ESI) m/z 585.40 ($\text{M} + \text{Na}$) $^+$.

2-((tert-Butoxycarbonyl)amino)ethyl ((2S,3R)-3-Hydroxy-4-(4-methoxy-N-pentylphenylsulfonamido)-1-phenylbutan-2-yl)carbamate (15e). The title compound was obtained from 12c and 7e as described for 13a in 62% yield after flash chromatography (1:3 EtOAc/hexane) as a colorless viscous liquid. ^1H NMR (400 MHz, CDCl_3) δ 7.64 (d, $J = 8.5$ Hz, 2H), 7.26–7.13 (m, 5H), 6.90 (d, $J = 9.2$ Hz, 2H), 5.03–4.76 (m, 1H), 4.68 (bs, 1H), 3.99–3.87 (m, 2H), 3.85–3.73 (m, 5H), 3.66–3.59 (m, 1H), 3.44–2.92 (m, 7H), 2.89–2.78 (m, 1H), 1.46–1.31 (m, 10H), 1.25–1.06 (m, 5H), 0.78 (t, $J = 7.3$ Hz, 3H); ^{13}C NMR (100 MHz, CDCl_3) δ 162.98, 156.36, 155.78, 137.67, 130.23, 129.46 (2C), 129.32 (2C), 128.49 (2C), 126.54, 114.32 (2C), 79.48, 72.20, 64.23, 55.59, 55.07, 52.27, 50.43, 39.93, 35.27, 28.74, 28.34 (3C), 28.17, 22.17, 13.90; MS (ESI) m/z 630.53 ($\text{M} + \text{Na}$) $^+$.

(R)-Methyl 3-(((2S,3R)-3-Hydroxy-4-(4-methoxy-N-pentylphenylsulfonamido)-1-phenylbutan-2-yl)carbamoyl)oxy)-2-methylpropanoate (15f). The title compound was obtained from 12c and 7f as described for 13a in 61% yield after flash chromatography (1:3 EtOAc/hexane) as an amorphous white solid. ^1H NMR (400 MHz, CDCl_3) δ 7.66–7.60 (m, 2H), 7.25–7.11 (m, 5H), 6.92–6.86 (m, 2H), 4.87 (d, $J = 7.9$ Hz, 1H), 4.09–3.97 (m, 2H), 3.83–3.71 (m, 5H), 3.69–3.61 (m, 1H), 3.57 (s, 3H), 3.11–2.90 (m, 4H), 2.87–2.78 (m, 1H), 2.68–2.56 (m, 1H), 1.45–1.34 (m, 2H), 1.24–1.07 (m, 5H), 1.04 (d, $J = 7.3$ Hz, 3H), 0.77 (t, $J = 7.0$ Hz, 3H); ^{13}C NMR (100 MHz, CDCl_3) δ 174.25, 162.93, 156.18, 137.55, 130.21, 129.44 (2C), 129.30 (2C), 128.45 (2C), 126.43, 114.27 (2C), 72.22, 65.99, 55.56, 55.01, 52.36, 51.80, 50.45, 39.24, 35.31, 28.71, 28.18, 22.14, 13.87, 13.52; MS (ESI) m/z 587.36 ($\text{M} + \text{Na}$) $^+$.

2-(2-Oxoimidazolidin-1-yl)ethyl ((2S,3R)-3-Hydroxy-4-(4-methoxy-N-pentylphenylsulfonamido)-1-phenylbutan-2-yl)carbamate (15g). The title compound was obtained from 12c and 7g as described for 13a in 70% yield after flash chromatography (1:3 EtOAc/hexane) as a white solid. ^1H NMR (400 MHz, CDCl_3) δ 7.66 (d, $J = 9.2$ Hz, 2H), 7.24–7.10 (m, 5H), 6.89 (d, $J = 9.2$ Hz, 2H), 5.16 (d, $J = 8.5$ Hz, 1H), 4.75 (bs, 1H), 4.14–4.02 (m, 2H), 3.95–3.89 (m, 1H), 3.86–3.79 (m, 2H), 3.78 (s, 3H), 3.39–3.13 (m, 5H), 3.05–2.99 (m, 1H), 2.95–2.71 (m, 3H), 2.68–2.59 (m, 1H), 1.54–1.26 (m, 2H), 1.23–0.99 (m, 6H), 0.73 (t, $J = 7.3$ Hz, 3H); ^{13}C NMR (100 MHz, CDCl_3) δ 162.94, 162.74, 156.23, 137.92, 130.61, 129.41 (2C), 129.37 (2C), 128.49 (2C), 126.45, 114.31 (2C), 71.94, 62.12, 55.64, 55.09, 51.84, 50.23, 45.27, 43.02, 38.20, 34.95, 28.84, 28.12, 22.24, 13.98; MS (ESI) m/z 599.38 ($\text{M} + \text{Na}$) $^+$.

2-(2-Oxooxazolidin-3-yl)ethyl ((2S,3R)-3-Hydroxy-4-(4-methoxy-N-pentylphenylsulfonamido)-1-phenylbutan-2-yl)carbamate (15h). The title compound was obtained from 12c and 7h as described for 13a in 67% yield after flash chromatography (1:3 EtOAc/hexane) as a colorless semisolid. ^1H NMR (400 MHz, CDCl_3) δ 7.71–7.67 (m, 2H), 7.27–7.17 (m, 5H), 6.96–6.62 (m, 2H), 5.10 (d, $J = 8.2$ Hz, 1H), 4.25–4.12 (m, 3H), 3.92–3.78 (m, 5H), 3.74–3.65 (m, 1H), 3.52–3.31 (m, 4H), 3.21–2.95 (m, 5H), 2.92–2.79 (m, 1H), 1.59–1.42 (m, 2H), 1.28–1.12 (m, 5H), 0.82 (t, $J = 6.7$ Hz, 3H); ^{13}C NMR (100 MHz, CDCl_3) δ 162.92, 158.59, 155.98, 137.77, 130.40, 129.36, 129.31 (3C), 128.41 (2C), 126.40, 114.29 (2C), 71.94, 61.87, 55.57, 55.14, 51.93, 50.28, 44.85, 43.68, 38.84, 35.17, 28.75, 28.11, 22.16, 13.90; MS (ESI) m/z 599.86 ($\text{M} + \text{Na}$) $^+$.

(R)-2-Oxotetrahydrofuran-3-yl ((2S,3R)-3-Hydroxy-4-(4-methoxy-N-pentylphenylsulfonamido)-1-phenylbutan-2-yl)carbamate (15i). The title compound was obtained from 12c and 7i as described for 13a in 50% yield after flash chromatography (1:3 EtOAc/hexane) as a colorless semisolid. ^1H NMR (400 MHz, CDCl_3) δ 7.76–7.69 (m, 2H), 7.30–7.15 (m, 5H), 7.01–6.96 (m, 2H), 4.62 (t, $J = 5.5$ Hz, 1H), 4.53–4.41 (m, 1H), 4.34–4.21 (m, 1H), 3.87 (s, 3H), 3.78–3.64 (m, 2H), 3.36–3.18 (m, 3H), 3.17–3.00 (m, 3H), 2.14–1.76 (m, 3H), 1.54–1.40 (m, 2H), 1.31–1.10 (m, 5H), 0.85 (t, $J = 7.3$ Hz, 3H); ^{13}C NMR (100 MHz, CDCl_3) δ 173.80, 163.01, 155.67, 136.72, 130.40, 129.43 (2C), 129.09 (2C), 128.65 (2C), 127.00, 114.34 (2C), 76.38, 70.99, 57.19, 56.88, 56.64, 51.69, 50.34, 32.36, 32.15, 28.77, 28.17, 22.21, 13.95; MS (ESI) m/z 571.34 ($\text{M} + \text{Na}$) $^+$.

(S)-5-Oxopyrrolidin-2-ylmethyl ((2S,3R)-3-Hydroxy-4-(4-methoxy-N-pentylphenylsulfonamido)-1-phenylbutan-2-yl)carbamate (15j). The title compound was obtained from 12c and 7j as described for 13a in 56% yield after flash chromatography (1:3 EtOAc/hexane) as a white solid. ^1H NMR (400 MHz, CDCl_3) δ 7.65 (d, $J = 8.5$ Hz, 2H), 7.23–7.09 (m, 5H), 6.93–6.86 (m, 3H), 5.47 (d, $J = 7.9$ Hz, 1H), 4.10–3.93 (m, 2H), 3.91–3.81 (m, 2H), 3.81–3.70 (m, 4H), 3.65 (dd, $J = 11.0, 7.3$ Hz, 1H), 3.16–2.99 (m, 3H), 2.94 (dd, $J = 14.0, 4.3$ Hz, 1H), 2.82–2.71 (m, 1H), 2.31–2.15 (m, 2H), 2.14–2.02 (m, 1H), 1.66–1.53 (m, 1H), 1.51–1.29 (m, 2H), 1.26–1.03 (m, 5H), 0.77 (t, $J = 6.9$ Hz, 3H); ^{13}C NMR (100 MHz, CDCl_3) δ 178.75, 162.92, 156.03, 138.96, 129.91, 129.56 (2C), 129.49 (2C), 128.36 (2C), 126.43, 114.30 (2C), 71.27, 66.36, 54.61, 54.25, 52.35, 50.85, 49.11, 36.03, 28.74, 27.81, 27.02, 21.86, 21.21, 13.06; MS (ESI) m/z 583.88 ($\text{M} + \text{Na}$) $^+$.

(R)-Methyl 3-(((2S,3R)-3-Hydroxy-4-(N-pentylbenzo[d]thiazole-6-sulfonamido)-1-phenylbutan-2-yl)carbamoyl)oxy)-

butanoate (16a). The title compound was obtained from **12d** and **7a** as described for **13a** in 51% yield after flash chromatography (1:2 EtOAc/hexane) as a colorless semisolid. $^1\text{H NMR}$ (400 MHz, CDCl_3) δ 9.14 (s, 1H), 8.43 (d, $J = 1.8$ Hz, 1H), 8.18 (d, $J = 8.5$ Hz, 1H), 7.87 (dd, $J = 8.5, 1.8$ Hz, 1H), 7.26–7.11 (m, 5H), 6.03 (d, $J = 8.5$ Hz, 1H), 5.21–5.11 (m, 1H), 4.18–4.09 (m, 2H), 3.87–3.79 (m, 1H), 3.60 (s, 3H), 3.29 (dd, $J = 14.6, 4.8$ Hz, 1H), 3.06–2.86 (m, 3H), 2.62–2.50 (m, 1H), 2.45–2.21 (m, 2H), 1.50–1.36 (m, 2H), 1.24–1.03 (m, 8H), 0.76 (t, $J = 7.3$ Hz, 3H); $^{13}\text{C NMR}$ (100 MHz, CDCl_3) δ 172.27, 170.75, 157.86, 155.49, 137.77, 136.30, 134.32, 129.30 (2C), 128.60 (2C), 126.62, 124.78, 124.33, 122.16, 72.18, 67.62, 54.68, 51.81, 50.39, 40.34, 35.13, 29.66, 28.79, 28.21, 22.18, 19.75, 13.90; MS (ESI) m/z 614.26 ($\text{M} + \text{Na}$) $^+$.

2-(2,2-Trifluoroacetamido)ethyl ((2S,3R)-3-Hydroxy-4-(N-pentylbenzo[d]thiazole-6-sulfonamido)-1-phenylbutan-2-yl)-carbamate (16b). The title compound was obtained from **12d** and **7b** as described for **13a** in 63% yield after flash chromatography (1:2 EtOAc/hexane) as a white solid. $^1\text{H NMR}$ (400 MHz, CDCl_3) δ 9.14 (s, 1H), 8.40 (d, $J = 1.8$ Hz, 1H), 8.17 (d, $J = 8.5$ Hz, 1H), 7.85–7.80 (m, 2H), 7.23–7.13 (m, 5H), 4.30 (t, $J = 7.9$ Hz, 2H), 4.08–4.00 (m, 1H), 3.88–3.80 (m, 3H), 3.51 (d, $J = 3.1$ Hz, 1H), 3.21–2.98 (m, 5H), 1.50–1.37 (m, 2H), 1.22–0.99 (m, 6H), 0.73 (t, $J = 7.3$ Hz, 3H); $^{13}\text{C NMR}$ (100 MHz, CDCl_3) δ 157.92, 155.49, 155.44, 152.86, 137.28, 136.17, 134.31, 129.44 (2C), 128.51 (3C), 126.66, 124.78, 124.35, 122.22, 72.02, 62.28, 54.95, 52.11, 50.36, 42.31, 35.89, 28.71, 28.19, 22.15, 13.88; MS (ESI) m/z 653.37 ($\text{M} + \text{Na}$) $^+$.

2-(2,2-Dichloroacetamido)ethyl ((2S,3R)-3-Hydroxy-4-(N-pentylbenzo[d]thiazole-6-sulfonamido)-1-phenylbutan-2-yl)-carbamate (16c). The title compound was obtained from **12d** and **7c** as described for **13a** in 58% yield after flash chromatography (1:2 EtOAc/hexane) as an amorphous white solid. $^1\text{H NMR}$ (400 MHz, CDCl_3) δ 9.14 (s, 1H), 8.44–8.33 (m, 1H), 8.20–8.15 (m, 1H), 7.83 (dd, $J = 9.2, 1.8$ Hz, 1H), 7.27–7.10 (m, 5H), 6.97 (bs, 1H), 5.91–5.78 (m, 1H), 5.08 (d, $J = 9.2$ Hz, 1H), 4.09–3.97 (m, 2H), 3.92–3.81 (m, 2H), 3.68–3.53 (m, 1H), 3.49–3.23 (m, 3H), 3.16–2.81 (m, 3H), 1.53–1.25 (m, 2H), 1.23–0.99 (m, 6H), 0.73 (t, $J = 7.3$ Hz, 3H); $^{13}\text{C NMR}$ (100 MHz, CDCl_3) δ 163.47, 157.12, 155.61, 154.64, 136.62, 135.22, 133.48, 128.51 (2C), 127.68 (2C), 125.80, 123.81, 123.51, 121.23, 71.21, 65.36, 62.22, 54.38, 51.23, 49.45, 39.37, 34.43, 27.83, 27.27, 21.26, 12.98; MS (ESI) m/z 666.92 ($\text{M} - 1 + \text{Na}$) $^+$, 668.93 ($\text{M} + 1 + \text{Na}$) $^+$.

(R)-5-Oxohexan-2-yl ((2S,3R)-3-Hydroxy-4-(N-pentylbenzo[d]thiazole-6-sulfonamido)-1-phenylbutan-2-yl)carbamate (16d). The title compound was obtained from **12d** and **7d** as described for **13a** in 65% yield after flash chromatography (1:2 EtOAc/hexane) as an amorphous white solid. $^1\text{H NMR}$ (400 MHz, CDCl_3) δ 9.14 (s, 1H), 8.40 (d, $J = 1.8$ Hz, 1H), 8.17 (d, $J = 8.5$ Hz, 1H), 7.83 (dd, $J = 8.5, 1.8$ Hz, 1H), 7.23–7.06 (m, 5H), 4.81 (d, $J = 8.5$ Hz, 1H), 4.64–4.56 (m, 1H), 3.92–3.67 (m, 3H), 3.21–3.04 (m, 1H), 3.01–2.92 (m, 1H), 2.89–2.79 (m, 2H), 2.35 (t, $J = 7.3$ Hz, 1H), 2.01 (s, 3H), 1.76–1.59 (m, 2H), 1.48–1.36 (m, 2H), 1.33–1.25 (m, 2H), 1.23–1.03 (m, 5H), 1.02 (d, $J = 6.1$ Hz, 3H), 0.79 (t, $J = 7.2$ Hz, 3H); $^{13}\text{C NMR}$ (100 MHz, CDCl_3) δ 207.99, 157.92, 156.35, 155.45, 137.68, 136.24, 134.28, 129.37 (2C), 128.46 (2C), 126.50, 124.68, 124.31, 122.07, 72.17, 71.01, 55.08, 52.07, 50.24, 39.44, 35.13, 29.81, 29.78, 28.69, 28.14, 22.11, 20.13, 13.84; MS (ESI) m/z 612.43 ($\text{M} + \text{Na}$) $^+$.

2-(tert-Butoxycarbonylamino)ethyl ((2S,3R)-3-Hydroxy-4-(N-pentylbenzo[d]thiazole-6-sulfonamido)-1-phenylbutan-2-yl)carbamate (16e). The title compound was obtained from **12d** and **7e** as described for **13a** in 54% yield after flash chromatography (1:2 EtOAc/hexane) as a white solid. $^1\text{H NMR}$ (400 MHz, CDCl_3) δ 9.14 (s, 1H), 8.39 (m, 1H), 8.14 (d, $J = 8.5$ Hz, 1H), 7.82 (dd, $J = 8.5, 1.8$ Hz, 1H), 7.22–7.09 (m, 5H), 4.85 (d, $J = 6.7$ Hz, 1H), 4.65 (bs, 1H), 3.97–3.88 (m, 2H), 3.85–3.76 (m, 2H), 3.70–2.62 (m, 1H), 3.29–3.02 (m, 6H), 3.01–2.92 (m, 1H), 2.88–2.78 (m, 1H), 1.49–1.32 (m, 10H), 1.23–1.05 (m, 5H), 0.75 (t, $J = 7.3$ Hz, 3H); $^{13}\text{C NMR}$ (100 MHz, CDCl_3) δ 157.94, 156.38, 155.79, 155.50, 137.59, 136.14, 134.33, 129.43 (2C), 128.56 (2C), 126.64, 124.72, 123.37, 122.12, 79.32, 72.13, 64.34, 55.17, 52.23, 50.38, 39.93, 35.22, 28.85, 28.24 (3C), 28.04, 22.16, 13.87; MS (ESI) m/z 657.36 ($\text{M} + \text{Na}$) $^+$.

(R)-Methyl 3-(((2S,3R)-3-Hydroxy-4-(N-pentylbenzo[d]thiazole-6-sulfonamido)-1-phenylbutan-2-yl)carbamoyloxy)-2-methylpropanoate (16f). The title compound was obtained from **12d** and **7f** as described for **13a** in 48% yield after flash chromatography (1:2 EtOAc/hexane) as a white solid. $^1\text{H NMR}$ (400 MHz, CDCl_3) δ 9.14 (s, 1H), 8.39 (d, $J = 1.8$ Hz, 1H), 8.17 (d, $J = 8.5$ Hz, 1H), 7.82 (dd, $J = 8.5, 1.8$ Hz, 1H), 7.26–7.12 (m, 6H), 4.92–4.81 (m, 1H), 4.09–3.98 (m, 2H), 3.93–3.51 (m, 3H), 3.57 (s, 3H), 3.19–3.02 (m, 3H), 2.99–2.93 (m, 1H), 2.89–2.81 (m, 1H), 2.68–2.59 (m, 1H), 1.47–1.36 (m, 1H), 1.22–1.08 (m, 5H), 1.04 (d, $J = 7.3$ Hz, 3H), 0.77 (t, $J = 7.0$ Hz, 3H); $^{13}\text{C NMR}$ (100 MHz, CDCl_3) δ 174.26, 157.94, 156.25, 155.47, 137.49, 136.10, 134.29, 129.42 (2C), 128.51 (2C), 126.56, 124.71, 124.31, 122.11, 72.23, 66.06, 55.15, 52.31, 51.81, 50.40, 39.26, 35.32, 28.68, 28.22, 22.12, 13.84, 13.51; MS (ESI) m/z 614.36 ($\text{M} + \text{Na}$) $^+$.

2-(2-Oxoimidazolidin-1-yl)ethyl ((2S,3R)-3-Hydroxy-4-(N-pentylbenzo[d]thiazole-6-sulfonamido)-1-phenylbutan-2-yl)-carbamate (16g). The title compound was obtained from **12d** and **7g** as described for **13a** in 57% yield after flash chromatography (1:2 EtOAc/hexane) as a white solid. $^1\text{H NMR}$ (400 MHz, CDCl_3) δ 9.13 (s, 1H), 8.42 (d, $J = 1.2$ Hz, 1H), 8.14 (d, $J = 8.5$ Hz, 1H), 7.84 (dd, $J = 8.5, 1.8$ Hz, 1H), 7.21–7.08 (m, 6H), 5.54 (d, $J = 8.5$ Hz, 1H), 5.11 (s, 1H), 4.17–4.06 (m, 1H), 3.97–3.80 (m, 3H), 3.50–3.41 (m, 1H), 3.38–3.18 (m, 4H), 3.18–3.01 (m, 3H), 3.00–2.87 (m, 1H), 2.79–2.65 (m, 1H), 1.54–1.33 (m, 2H), 1.23–0.99 (m, 6H), 0.73 (t, $J = 7.3$ Hz, 3H); $^{13}\text{C NMR}$ (100 MHz, CDCl_3) δ 162.92, 158.00, 156.06, 155.22, 137.97, 136.43, 134.13, 129.18 (2C), 128.24 (2C), 126.20, 124.67, 124.05, 122.03, 71.78, 61.67, 55.10, 51.39, 49.72, 42.74, 38.05, 34.73, 28.62, 27.77, 25.32, 22.01, 13.76; MS (ESI) m/z 626.34 ($\text{M} + \text{Na}$) $^+$.

2-(2-Oxooxazolidin-3-yl)ethyl ((2S,3R)-3-Hydroxy-4-(N-pentylbenzo[d]thiazole-6-sulfonamido)-1-phenylbutan-2-yl)-carbamate (16h). The title compound was obtained from **12d** and **7h** as described for **13a** in 66% yield after flash chromatography (1:2 EtOAc/hexane) as a white solid. $^1\text{H NMR}$ (400 MHz, CDCl_3) δ 9.18 (s, 1H), 8.47 (d, $J = 1.8$ Hz, 1H), 8.23–8.20 (m, 1H), 7.92–7.89 (m, 1H), 7.29–7.18 (m, 6H), 5.01 (d, $J = 7.3$ Hz, 1H), 4.23–4.17 (m, 2H), 4.05–3.81 (m, 3H), 3.69 (bs, 1H), 3.52–3.34 (m, 4H), 3.29–3.10 (m, 3H), 3.07–2.97 (m, 1H), 2.92–2.78 (m, 1H), 1.57–1.41 (m, 2H), 1.29–1.10 (m, 5H), 0.81 (t, $J = 4.9$ Hz, 3H); $^{13}\text{C NMR}$ (100 MHz, CDCl_3) δ 158.72, 158.04, 156.08, 155.46, 137.81, 136.43, 134.33, 129.37 (2C), 128.49 (2C), 126.50, 124.82, 124.29, 122.19, 71.83, 61.93, 55.29, 51.80, 50.16, 44.70, 43.72, 35.14, 29.26, 28.77, 28.18, 22.19, 13.92; MS (ESI) m/z 626.85 ($\text{M} + \text{Na}$) $^+$.

(R)-2-Oxotetrahydrofuran-3-yl ((2S,3R)-3-Hydroxy-4-(N-pentylbenzo[d]thiazole-6-sulfonamido)-1-phenylbutan-2-yl)-carbamate (16i). The title compound was obtained from **12d** and **7i** as described for **13a** in 53% yield after flash chromatography (1:2 EtOAc/hexane) as an amorphous white solid. $^1\text{H NMR}$ (400 MHz, CDCl_3) δ 9.14 (s, 1H), 8.42 (d, $J = 1.8$ Hz, 1H), 8.14 (d, $J = 8.5$ Hz, 1H), 7.85 (dd, $J = 8.5, 1.8$ Hz, 1H), 7.23–7.09 (m, 5H), 4.55 (t, $J = 5.6$ Hz, 1H), 4.42–4.34 (m, 1H), 4.30–4.21 (m, 1H), 3.77 (dd, $J = 3.7, 9.2$ Hz, 1H), 3.70–3.57 (m, 2H), 3.37–3.30 (m, 1H), 3.29–3.16 (m, 2H), 3.15–3.06 (m, 3H), 2.02–1.90 (m, 1H), 1.89–1.75 (m, 1H), 1.50–1.35 (m, 2H), 1.23–1.04 (m, 5H), 0.76 (t, $J = 7.8$ Hz, 3H); $^{13}\text{C NMR}$ (100 MHz, CDCl_3) δ 173.78, 158.11, 155.60, 155.35, 136.58, 136.32, 134.27, 129.03 (2C), 128.61 (2C), 126.99, 124.73, 124.25, 122.23, 76.35, 70.88, 57.04, 56.82, 51.61, 50.22, 32.35, 28.69, 28.08, 22.13, 14.15, 13.84; MS (ESI) m/z 598.13 ($\text{M} + \text{Na}$) $^+$.

(S)-5-Oxopyrrolidin-2-ylmethyl ((2S,3R)-3-Hydroxy-4-(N-pentylbenzo[d]thiazole-6-sulfonamido)-1-phenylbutan-2-yl)-carbamate (16j). The title compound was obtained from **12d** and **7j** as described for **13a** in 68% yield after flash chromatography (1:2 EtOAc/hexane) as foam. $^1\text{H NMR}$ (400 MHz, CDCl_3) δ 9.12 (s, 1H), 8.40 (s, 1H), 8.14 (d, $J = 8.5$ Hz, 1H), 7.83 (d, $J = 8.5$ Hz, 1H), 7.25–7.08 (m, 6H), 4.36–4.00 (m, 2H), 3.96–3.68 (m, 3H), 3.66–3.53 (m, 1H), 3.31–3.05 (m, 4H), 2.99–2.87 (m, 1H), 2.83–2.66 (m, 1H), 2.30–1.99 (m, 3H), 1.67–1.30 (m, 3H), 1.25–1.04 (m, 5H), 0.72 (t, $J = 6.8$ Hz, 3H); $^{13}\text{C NMR}$ (100 MHz, CDCl_3) δ 178.89, 157.96, 155.92, 155.34, 137.86, 136.45, 134.22, 129.27 (2C), 128.37 (2C), 126.41, 124.73, 124.16, 122.07, 71.81, 67.28, 55.21, 53.29, 51.58,

49.84, 34.82, 29.71, 28.68, 27.88, 22.72, 22.09, 13.81; MS (ESI) m/z 611.29 ($M + Na$)⁺.

HIV-1 Protease Inhibition Assays. The protease inhibitory activities were determined by a fluorescence resonance energy transfer (FRET) method^{22,23,34} in a semi-high-throughput format. Protease substrate (Arg-Glu(EDANS)-Ser-Gln-Asn-Tyr-Pro-Ile-Val-Gln Lys-(DABCYL)-Arg) was purchased from Molecular Probes. The expression, isolation, and purification of wild-type and mutant HIV-1 protease used for binding experiments were carried out as previously described.³⁹ Wild-type HIV-1 protease (Q7K) and its MDR variants (L10I, G48V, I54V, L63P, V82A for M1; L10I, L63P, A71V, G73S, I84V, L90M for M2; I50V, A71V for M3) were desalted through PD-10 columns (Amersham Biosciences). Sodium acetate (20 mM, pH 5) was used as the elution buffer. Apparent protease concentrations were around ~50 nM as estimated by UV spectrophotometry at 280 nm. Fluorescence measurements were carried out on EnVisioin plate reader (PerkinElmer). Excitation and emission filters were 340 and 492 nm, respectively. All inhibitors were dissolved in DMSO and diluted to 12 appropriate concentrations in 96-well plate (8 inhibitors/plate). Protease (2 μ L) and inhibitor or DMSO (1 μ L) were added into a half-area 96-well assay plate containing 37 μ M HIV-1 substrate buffer [0.1 M sodium acetate, 1 M sodium chloride, 1 mM ethylenediaminetetraacetic acid (EDTA), 1 mM dithiothreitol (DTT), 2% DMSO, and 1 mg/mL bovine serum albumin (BSA) with an adjusted pH of 4.7]. All pipetting was performed by a liquid handling system (Tecan Genesis and TeMo). Protease substrate (40 μ L) was quickly injected into the assay plate with one row at a time by Envision injector to initiate the cleavage reaction. Each reaction was recorded for 5 min. Inhibitor binding dissociation constant (K_i) values were obtained by nonlinear regression fitting (GraFit 5, Erithacus Software) of the plot of initial velocity as a function of inhibitor concentrations based on the Morrison equation.⁴⁰ The initial velocities were derived from the linear range of reaction curves.

Antiviral Assays. Drug susceptibility assays were carried out by Monogram Biosciences against three patient-derived strains of wild-type HIV-1 from clades A, B, and C and against two multidrug-resistant HIV-1 variants. Assays were carried out according to protocols detailed by Petropoulos et al.⁴¹ and on the Web site <http://www.monogramvirology.com>. Genbank accession numbers for the PR/RT regions of the six HIV-1 strains used in antiviral assays are as follows: WT-control, HQ179654; WT-A, HQ179655; WT-B, HQ179656; WT-C, HQ179657; MDR, HQ179658; MDR1, HQ179659.

Protein Crystallography. The expression, isolation, and purification of wild-type HIV-1 protease used for crystallization experiments were carried out as previously described.³⁹ Cocrystals of the inhibitors with the wild-type protease were grown at room temperature by hanging drop vapor diffusion method. Protease concentration of 1.6 mg/mL was used with 3-fold molar excess of inhibitors to set the crystallization drops. The reservoir solution consisted of 126 mM phosphate buffer at pH 6.2, 63 mM sodium citrate, and 24–29% ammonium sulfate.

The crystals used for data collection were mounted in Mitegen Micromounts and flash-frozen over a nitrogen stream. Intensity data for **13c** wild-type protease complex were collected at -80 °C on an in-house Rigaku X-ray generator equipped with an R-axis IV image plate. Then 180 frames were collected per crystal with an angular separation of 1° and no overlap between frames. Intensity data for protease complexes of **13g**, **13f**, and **14j** were collected under cryogenic conditions at BioCARS 14-BMC beamline at Argonne National Laboratory (Advanced Photon Source, Chicago, IL). Diffraction images for all four complexes were indexed and scaled using the program HKL2000.⁴²

The crystal structures were solved and refined with the programs within the CCP4 interface.⁴³ Structure solutions for all the wild-type protease–inhibitor complexes were obtained with the molecular replacement package AMoRe⁴⁴ using 1F7A⁴⁵ as the starting model. Model building was performed using the interactive graphics program Coot.⁴⁶ Conjugate gradient refinement using Refmac5⁴⁷ was performed by incorporating Schomaker and Trueblood tensor

formulation of TLS (translation, libration, screw–rotation) parameters.^{48–50} The working R (R_{factor}) and its cross-validation (R_{free}) were monitored throughout the refinement. The data collection and refinement statistics are shown in Table 4.

Table 4. X-ray Crystallographic Data Collection and Refinement Statistics for Complexes of 13c, 13f, 13g, and 14j with the Wild-Type HIV-1 Protease

	13c	13f	13g	14j
resolution (Å)	1.78	1.40	1.40	1.55
space group	$P2_12_12_1$	$P2_12_12_1$	$P2_12_12_1$	$P2_12_12_1$
<i>a</i> (Å)	50.73	50.83	50.71	50.73
<i>b</i> (Å)	57.76	57.97	57.93	57.85
<i>c</i> (Å)	61.74	62.00	61.82	61.69
<i>Z</i>	4	4	4	4
R_{merge} (%)	4.3	5.9	5.4	5.6
completeness (%)	98.7	99.6	99.1	97.9
total no. of reflections	121 403	252 434	244 283	169 795
no. of unique reflections	17 839	36 681	36 239	26 519
R_{free} (%)	21.7	18.9	20.4	19.6
R_{factor} (%)	16.0	17.3	17.9	17.0
rmsd bond length (Å)	0.009	0.009	0.009	0.009
rms angle (deg)	1.310	1.296	1.368	1.393
temperature (°C)	−80	−80	−80	−80
PDB code	4DJO	4DJP	4DJQ	4DJR

■ ASSOCIATED CONTENT

📄 Supporting Information

Detailed experimental procedures for the synthesis of intermediate activated carbonates (**7a–j**), (*R*)-hydroxyethylamines (**10a,b**), and (*R*)-(hydroxyethylamino)sulfonamides (**12a–d**), characterization data for intermediates, and results of HPLC analysis for all final compounds. This material is available free of charge via the Internet at <http://pubs.acs.org>.

■ AUTHOR INFORMATION

Corresponding Author

*Phone: (858) 795-5325. Fax: (858) 795-5328. E-mail: trana@sanfordburnham.org.

Notes

The authors declare no competing financial interest.

■ ACKNOWLEDGMENTS

This research was supported in part by grants from the National Institutes of General Medical Sciences of the NIH (Grants GM066524, GM082209, AI41404, AI43198). We thank Kaneka USA for their generous gifts of chiral epoxides, Ellen A. Nalivaika for providing the wild-type and MDR HIV-1 proteases, the AIDS Research and Reference Reagent Program (NIAD, NIH) for reference protease inhibitors, Monogram Biosciences for antiviral testing, and members of the Rana, Tidor, and Schiffer laboratories for helpful discussions, particularly Dr. Huricha Baigude for his help in HPLC data collection. In addition, we thank Kuan Hung Lin for his help in the refinement of the wild-type protease complex of **13c** and Shivender Shandilya for collecting the data on complexes of **13f**, **13g**, and **14j** with the wild-type protease at BioCARS beamline of the Advanced Photon Source, Argonne National Laboratory, IL. Use of the Advanced Photon Source for X-ray data collection was supported by the U.S. Department of Energy, Basic Energy Sciences, Office of Science, under

Contract DE-AC02-06CH11357. Use of the BioCARS Sector 14 was supported by the National Institutes of Health, National Center for Research Resources, under Grant RR007707.

REFERENCES

- (1) Bartlett, J. A.; DeMasi, R.; Quinn, J.; Moxham, C.; Rousseau, F. Overview of the effectiveness of triple combination therapy in antiretroviral-naive HIV-1 infected adults. *AIDS* **2001**, *15*, 1369–1377.
- (2) Gulick, R. M.; Mellors, J. W.; Havlir, D.; Eron, J. J.; Meibohm, A.; Condra, J. H.; Valentine, F. T.; McMahon, D.; Gonzalez, C.; Jonas, L.; Emini, E. A.; Chodakewitz, J. A.; Isaacs, R.; Richman, D. D. 3-Year suppression of HIV viremia with indinavir, zidovudine, and lamivudine. *Ann. Intern. Med.* **2000**, *133*, 35–39.
- (3) Palella, F. J.; Delaney, K. M.; Moorman, A. C.; Loveless, M. O.; Fuhrer, J.; Satten, G. A.; Aschman, D. J.; Holmberg, S. D. The, H. I. V. O. S. I. Declining morbidity and mortality among patients with advanced human immunodeficiency virus infection. *N. Engl. J. Med.* **1998**, *338*, 853–860.
- (4) Hogg, R. S.; Heath, K. V.; Yip, B.; Craib, K. J. P.; O'Shaughnessy, M. V.; Schechter, M. T.; Montaner, J. S. G. Improved survival among HIV-infected individuals following initiation of antiretroviral therapy. *JAMA, J. Am. Med. Assoc.* **1998**, *279*, 450–454.
- (5) Waters, L.; Nelson, M. Why do patients fail HIV therapy? *Int. J. Clin. Pract.* **2007**, *61*, 983–990.
- (6) Condra, J. H.; Schleif, W. A.; Blahy, O. M.; Gabryelski, L. J.; Graham, D. J.; Quintero, J. C.; Rhodes, A.; Robbins, H. L.; Roth, E.; Shivaprakash, M.; Titus, D.; Yang, T.; Tepplert, H.; Squires, K. E.; Deutsch, P. J.; Emini, E. A. In vivo emergence of HIV-1 variants resistant to multiple protease inhibitors. *Nature* **1995**, *374*, 569–571.
- (7) Clavel, F.; Hance, A. J. HIV drug resistance. *N. Engl. J. Med.* **2004**, *350*, 1023–1035.
- (8) Prabu-Jeyabalan, M.; Nalivaika, E.; Schiffer, C. A. Substrate shape determines specificity of recognition for HIV-1 protease: analysis of crystal structures of six substrate complexes. *Structure* **2002**, *10*, 369–381.
- (9) Kim, E. E.; Baker, C. T.; Dwyer, M. D.; Murcko, M. A.; Rao, B. G.; Tung, R. D.; Navia, M. A. Crystal structure of HIV-1 protease in complex with VX-478, a potent and orally bioavailable inhibitor of the enzyme. *J. Am. Chem. Soc.* **1995**, *117*, 1181–1182.
- (10) Koh, Y.; Nakata, H.; Maeda, K.; Ogata, H.; Bilcer, G.; Devasamudram, T.; Kincaid, J. F.; Boross, P.; Wang, Y.-F.; Tie, Y.; Volarath, P.; Gaddis, L.; Harrison, R. W.; Weber, I. T.; Ghosh, A. K.; Mitsuya, H. Novel bis-tetrahydrofuranylurethane-containing non-peptidic protease inhibitor (PI) UIC-94017 (TMC114) with potent activity against multi-PI-resistant human immunodeficiency virus in vitro. *Antimicrob. Agents Chemother.* **2003**, *47*, 3123–3129.
- (11) Surleraux, D. L. N. G.; Tahri, A.; Verschuere, W. G.; Pille, G. M. E.; de Kock, H. A.; Jonckers, T. H.; Peeters, A.; De Meyer, S.; Azijn, H.; Pauwels, R.; de Bethune, M.-P.; King, N. M.; Prabu-Jeyabalan, M.; Schiffer, C. A.; Wigerinck, P. B. T. P. Discovery and selection of TMC114, a next generation HIV-1 protease inhibitor. *J. Med. Chem.* **2005**, *48*, 1813–1822.
- (12) De Meyer, S.; Azijn, H.; Surleraux, D.; Jochmans, D.; Tahri, A.; Pauwels, R.; Wigerinck, P.; de Bethune, M. P. TMC114, a novel human immunodeficiency virus type 1 protease inhibitor active against protease inhibitor-resistant viruses, including a broad range of clinical isolates. *Antimicrob. Agents Chemother.* **2005**, *49*, 2314–2321.
- (13) King, N. M.; Prabu-Jeyabalan, M.; Nalivaika, E. A.; Wigerinck, P. B. T. P.; de Bethune, M. P.; Schiffer, C. A. Structural and thermodynamic basis for the binding of TMC114, a next-generation human immunodeficiency virus type 1 protease inhibitor. *J. Virol.* **2004**, *78*, 12012–12021.
- (14) Kovalevsky, A. Y.; Tie, Y.; Liu, F.; Boross, P. I.; Wang, Y.-F.; Leshchenko, S.; Ghosh, A. K.; Harrison, R. W.; Weber, I. T. Effectiveness of nonpeptide clinical inhibitor TMC-114 on HIV-1 protease with highly drug resistant mutations D30N, I50V, and L90M. *J. Med. Chem.* **2006**, *49*, 1379–1387.
- (15) Surleraux, D. L. N. G.; de Kock, H. A.; Verschuere, W. G.; Pille, G. M. E.; Maes, L. R.; Peeters, A.; Vendeville, S.; De Meyer, S.; Azijn, H.; Pauwels, R.; de Bethune, M. P.; King, N. M.; Prabu-Jeyabalan, M.; Schiffer, C. A.; Wigerinck, P. B. T. P. Design of HIV-1 protease inhibitors active on multidrug-resistant virus. *J. Med. Chem.* **2005**, *48*, 1965–1973.
- (16) Miller, J. F.; Andrews, C. W.; Brieger, M.; Furfine, E. S.; Hale, M. R.; Hanlon, M. H.; Hazen, R. J.; Kaldor, I.; McLean, E. W.; Reynolds, D.; Sammond, D. M.; Spaltenstein, A.; Tung, R.; Turner, E. M.; Xu, R. X.; Sherrill, R. G. Ultra-potent P1 modified arylsulfonamide HIV protease inhibitors: the discovery of GW0385. *Bioorg. Med. Chem. Lett.* **2006**, *16*, 1788–1794.
- (17) He, G.-X.; Yang, Z.-Y.; Williams, M.; Callebaut, C.; Cihlar, T.; Murray, B. P.; Yang, C.; Mitchell, M. L.; Liu, H.; Wang, J.; Arimilli, M.; Eisenberg, E.; Stray, K. M.; Tsai, L. K.; Hatada, M.; Chen, X.; Chen, J. M.; Wang, Y.; Lee, M. S.; Strickley, R. G.; Iwata, Q.; Zheng, X.; Kim, C. U.; Swaminathan, S.; Desai, M. C.; Lee, W. A.; Xu, L. Discovery of GS-8374, a potent human immunodeficiency virus type 1 protease inhibitor with a superior resistance profile. *MedChemComm* **2011**, *2*, 1093–1098.
- (18) Ghosh, A. K.; Sridhar, P. R.; Leshchenko, S.; Hussain, A. K.; Li, J.; Kovalevsky, A. Y.; Walters, D. E.; Wedekind, J. E.; Grum-Tokars, V.; Das, D.; Koh, Y.; Maeda, K.; Gatanaga, H.; Weber, I. T.; Mitsuya, H. Structure-based design of novel HIV-1 protease inhibitors to combat drug resistance. *J. Med. Chem.* **2006**, *49*, 5252–5261.
- (19) Ghosh, A. K.; Gemma, S.; Baldrige, A.; Wang, Y.-F.; Kovalevsky, A. Y.; Koh, Y.; Weber, I. T.; Mitsuya, H. Flexible cyclic ethers/polyethers as novel P2-ligands for HIV-1 protease inhibitors: design, synthesis, biological evaluation, and protein–ligand X-ray studies. *J. Med. Chem.* **2008**, *51*, 6021–6033.
- (20) Ghosh, A. K.; Chapsal, B. D.; Baldrige, A.; Steffey, M. P.; Walters, D. E.; Koh, Y.; Amano, M.; Mitsuya, H. Design and synthesis of potent HIV-1 protease inhibitors incorporating hexahydrofuro-pyr-anol-derived high affinity P2 ligands: structure–activity studies and biological evaluation. *J. Med. Chem.* **2011**, *54*, 622–634.
- (21) Ali, A.; Reddy, G. S. K. K.; Cao, H.; Anjum, S. G.; Nalam, M. N. L.; Schiffer, C. A.; Rana, T. M. Discovery of HIV-1 protease inhibitors with picomolar affinities incorporating N-aryl-oxazolidinone-5-carbox-amides as novel P2 ligands. *J. Med. Chem.* **2006**, *49*, 7342–7356.
- (22) Ali, A.; Reddy, G. S. K. K.; Nalam, M. N. L.; Anjum, S. G.; Cao, H.; Schiffer, C. A.; Rana, T. M. Structure-based design, synthesis, and structure–activity relationship studies of HIV-1 protease inhibitors incorporating phenyloxazolidinones. *J. Med. Chem.* **2010**, *53*, 7699–7708.
- (23) Altman, M. D.; Ali, A.; Reddy, G. S. K. K.; Nalam, M. N. L.; Anjum, S. G.; Cao, H.; Chellappan, S.; Kairys, V.; Fernandes, M. X.; Gilson, M. K.; Schiffer, C. A.; Rana, T. M.; Tidor, B. HIV-1 protease inhibitors from inverse design in the substrate envelope exhibit subnanomolar binding to drug-resistant variants. *J. Am. Chem. Soc.* **2008**, *130*, 6099–6113.
- (24) Brooks, B. R.; Brucoleri, R. E.; Olafson, B. D.; States, D. J.; Swaminathan, S.; Karplus, M. CHARMM: a program for macromolecular energy, minimization, and dynamics calculations. *J. Comput. Chem.* **1983**, *4*, 187–217.
- (25) Momany, F. A.; Rone, R. Validation of the general purpose QUANTA 3.2/CHARMM force field. *J. Comput. Chem.* **1992**, *13*, 888–900.
- (26) Sitkoff, D.; Sharp, K. A.; Honig, B. Accurate calculation of hydration free energies using macroscopic solvent models. *J. Phys. Chem.* **1994**, *98*, 1978–1988.
- (27) Gilson, M. K.; Honig, B. Calculation of the total electrostatic energy of a macromolecular system: solvation energies, binding energies, and conformational analysis. *Proteins* **1988**, *4*, 7–18.
- (28) Nicholls, A.; Honig, B. A rapid finite difference algorithm, utilizing successive over-relaxation to solve the Poisson–Boltzmann equation. *J. Comput. Chem.* **1991**, *12*, 435–445.
- (29) Kangas, E.; Tidor, B. Optimizing electrostatic affinity in ligand–receptor binding: theory, computation, and ligand properties. *J. Chem. Phys.* **1998**, *109*, 7522–7545.

(30) Gilson, M. K.; Sharp, K. A.; Honig, B. H. Calculating the electrostatic potential of molecules in solution: method and error assessment. *J. Comput. Chem.* **1988**, *9*, 327–335.

(31) Irwin, J. J.; Shoichet, B. K. ZINC: a free database of commercially available compounds for virtual screening. *J. Chem. Inf. Model.* **2005**, *45*, 177–182.

(32) Desmet, J.; Maeyer, M. D.; Hazes, B.; Lasters, I. The dead-end elimination theorem and its use in protein side-chain positioning. *Nature* **1992**, *356*, 539–542.

(33) Leach, A. R.; Lemon, A. P. Exploring the conformational space of protein side chains using dead-end elimination and the A* algorithm. *Proteins* **1998**, *33*, 227–239.

(34) Matayoshi, E. D.; Wang, G. T.; Krafft, G. A.; Erickson, J. Novel fluorogenic substrates for assaying retroviral proteases by resonance energy transfer. *Science* **1990**, *247*, 954–958.

(35) Wu, T. D.; Schiffer, C. A.; Gonzales, M. J.; Taylor, J.; Kantor, R.; Chou, S.; Israelski, D.; Zolopa, A. R.; Fessel, W. J.; Shafer, R. W. Mutation patterns and structural correlates in human immunodeficiency virus type 1 protease following different protease inhibitor treatments. *J. Virol.* **2003**, *77*, 4836–4847.

(36) Nalam, M. N. L.; Ali, A.; Altman, M. D.; Reddy, G. S. K. K.; Chellappan, S.; Kairys, V.; Ozen, A.; Cao, H.; Gilson, M. K.; Tidor, B.; Rana, T. M.; Schiffer, C. A. Evaluating the substrate-envelope hypothesis: structural analysis of novel HIV-1 protease inhibitors designed to be robust against drug resistance. *J. Virol.* **2010**, *84*, 5368–5378.

(37) Freire, E. Do enthalpy and entropy distinguish first in class from best in class? *Drug Discovery Today* **2008**, *13*, 869–874.

(38) Bissantz, C.; Kuhn, B.; Stahl, M. A medicinal chemist's guide to molecular interactions. *J. Med. Chem.* **2010**, *53*, 5061–5084.

(39) King, N. M.; Melnick, L.; Prabu-Jeyabalan, M.; Nalivaika, E. A.; Yang, S. S.; Gao, Y.; Nie, X.; Zepp, C.; Heefner, D. L.; Schiffer, C. A. Lack of synergy for inhibitors targeting a multi-drug-resistant HIV-1 protease. *Protein Sci.* **2002**, *11*, 418–429.

(40) Greco, W. R.; Hakala, M. T. Evaluation of methods for estimating the dissociation constant of tight binding enzyme inhibitors. *J. Biol. Chem.* **1979**, *254*, 12104–12109.

(41) Petropoulos, C. J.; Parkin, N. T.; Limoli, K. L.; Lie, Y. S.; Wrin, T.; Huang, W.; Tian, H.; Smith, D.; Winslow, G. A.; Capon, D. J.; Whitcomb, J. M. A novel phenotypic drug susceptibility assay for human immunodeficiency virus type 1. *Antimicrob. Agents Chemother.* **2000**, *44*, 920–928.

(42) Otwinowski, Z.; Minor, W.; Carter, C. W., Jr. Processing of X-ray diffraction data collected in oscillation mode. *Methods Enzymol.* **1997**, *276*, 307–326.

(43) Collaborative computational project, number 4. The CCP4 suite: programs for protein crystallography. *Acta Crystallogr.* **1994**, *D50*, 760–763.

(44) Navaza, J. AMoRe: an automated package for molecular replacement. *Acta Crystallogr.* **1994**, *A50*, 157–163.

(45) Prabu-Jeyabalan, M.; Nalivaika, E.; Schiffer, C. A. How does a symmetric dimer recognize an asymmetric substrate? A substrate complex of HIV-1 protease. *J. Mol. Biol.* **2000**, *301*, 1207–1220.

(46) Emsley, P.; Cowtan, K. Coot: model-building tools for molecular graphics. *Acta Crystallogr.* **2004**, *D60*, 2126–2132.

(47) Murshudov, G. N.; Vagin, A. A.; Dodson, E. J. Refinement of macromolecular structures by the maximum-likelihood method. *Acta Crystallogr.* **1997**, *D53*, 240–255.

(48) Schomaker, V.; Trueblood, K. N. On the rigid-body motion of molecules in crystals. *Acta Crystallogr.* **1968**, *B24*, 63–76.

(49) Kuriyan, J.; Weis, W. I. Rigid protein motion as a model for crystallographic temperature factors. *Proc. Natl. Acad. Sci. U.S.A.* **1991**, *88*, 2773–2777.

(50) Tickle, I. J.; Moss, D. S. Modeling Rigid-Body Thermal Motion in Macromolecular Crystal Structure Refinement. In *IUCr99 Computing School*; IUCr: London, 1999.